


Root cortex development is fine-tuned by the interplay of MIGs, SCL3 and DELLAs during arbuscular mycorrhizal symbiosis

Christine Seemann, Carolin Heck, Stefanie Voß, Jana Schmoll, Eileen Enderle, Diana Schwarz and Natalia Requena 

Molecular Phytopathology, Botanical Institute, Karlsruhe Institute of Technology (KIT), Fritz-Haber-Weg 4, D-76131, Karlsruhe, Germany

Author for correspondence:
Natalia Requena
Email: natalia.requena@kit.edu

Received: 10 June 2021
Accepted: 19 October 2021

New Phytologist (2021)
doi: 10.1111/nph.17823

Key words: arbuscular mycorrhiza, arbuscule, GRAS transcription factors, root development, symbiosis.

Summary

- Root development is a crucial process that determines the ability of plants to acquire nutrients, adapt to the substrate and withstand changing environmental conditions. Root plasticity is controlled by a plethora of transcriptional regulators that allow, in contrast to tissue development in animals, post-embryonic changes that give rise to new tissue and specialized cells.
- One of these changes is the accommodation in the cortex of hyperbranched hyphae of symbiotic arbuscular mycorrhizal (AM) fungi, called arbuscules. Arbuscule-containing cells undergo massive reprogramming to coordinate developmental changes with transport processes.
- Here we describe a novel negative regulator of arbuscule development, MIG3. MIG3 induces and interacts with SCL3, both of which modulate the activity of the central regulator DELLA, restraining cortical cell growth. As in a tug-of-war, MIG3-SCL3 antagonizes the function of the complex MIG1-DELLA, which promotes the cell expansion required for arbuscule development, adjusting cell size during the dynamic processes of the arbuscule life cycle.
- Our results in the legume plant *Medicago truncatula* advance the knowledge of root development in dicot plants, showing the existence of additional regulatory elements not present in *Arabidopsis* that fine-tune the activity of conserved central modules.

Introduction

Plants in natural ecosystems live in association with a multitude of microbes which, together with the environmental and soil conditions, shape plant health and growth. Among the most widespread and important microbes associated with plants are the arbuscular mycorrhizal (AM) fungi. These soil-borne fungi from the Glomeromycotina subphylum colonize the roots of most terrestrial plants, forming a symbiosis that dates back 460 Myr (Simon *et al.*, 1993; Remy *et al.*, 1994; Redecker *et al.*, 2000; Smith & Read, 2008; Spatafora *et al.*, 2016; Berbee *et al.*, 2017). Arbuscular mycorrhizal fungi are obligate biotrophs and feed on plant-fixed carbon (sugars and lipids), improving, in turn, plant mineral nutrition and water relations, notably by the delivery of phosphorous, but also nitrogen, iron, copper, manganese and zinc, to the plant (Smith & Smith, 2011). They are, thus, essential components of the terrestrial ecosystem contributing to the closing of nutrient cycles.

Arbuscular mycorrhizal fungal colonization of roots is limited to the rhizodermis and cortex. After entering between or through epidermal cells, fungal hyphae develop inter- and intracellularly, without disruption of the plasma membrane. It is remarkable that, despite the multitude of fungal and plant species that are

able to enter into AM symbiosis, the morphology of the colonization is relatively similar, with one common organ: the arbuscule. Arbuscules are located in deeper layers of the cortex in most plants and are tree-like structures formed by profuse dichotomous hyphal branching. Arbuscules reside in the cell lumen embedded in an apoplastic compartment and surrounded by the plant periarbuscular membrane (PAM). Periarbuscular membrane biogenesis requires an extensive exocytotic activity to generate the extensive membrane increase required to envelop hyphal branches and to secrete the plant transporters that will enable the nutrient uptake into the plant cytoplasm (Pumplin *et al.*, 2012). The arbuscule is the key organ of the AM symbiosis, and the process of its initiation, maturation and degradation requires a major transcriptional reprogramming that involves the exchange, perception and transmission of signals in both directions (Lanfranco *et al.*, 2018). This reprogramming is directed by a well-orchestrated ensemble of plant transcription factors – and presumably fungal transcription factors which have not yet been identified – that produce the morphological and developmental changes required for the formation of this highly specialized nutrient/signal exchange structure (Hohnjec *et al.*, 2005; Gomez *et al.*, 2009; Guether *et al.*, 2009; Gaude *et al.*, 2012; Gobato *et al.*, 2012; Wang *et al.*, 2012; Devers *et al.*, 2013; Floss

et al., 2013, 2017; Foo *et al.*, 2013; Volpe *et al.*, 2013; Park *et al.*, 2015; Xue *et al.*, 2015, 2018; Heck *et al.*, 2016; Pimprikar *et al.*, 2016; Luginbuehl *et al.*, 2017; Ho-Plagaro *et al.*, 2019; Russo *et al.*, 2019a; Choi *et al.*, 2020).

Discoveries from the last 10 yr have revealed that many of those transcription factors are members of the GRAS family. From these findings emerges a picture in which DELLA proteins are central regulators of arbuscule function, as they interact with multiple other transcription factors that have been shown to regulate arbuscule cell morphology and function (Floss *et al.*, 2013, 2016, 2017; Heck *et al.*, 2016; Pimprikar *et al.*, 2016). DELLAs are key interconnectors of hormonal and metabolic pathways, notably controlling the phosphate starvation response (Jiang *et al.*, 2007), and it is therefore not surprising that they are central to this symbiosis. DELLA proteins are degraded upon the binding of gibberellin (GA) to its receptor, and in the absence of GA, DELLA represses GA signaling. Gibberellin is known to inhibit arbuscule branching when applied to roots (El Ghachtouli *et al.*, 1996), and DELLA mutants in *Medicago truncatula*, pea and rice are impaired in arbuscule development (Floss *et al.*, 2013; Foo *et al.*, 2013; Yu *et al.*, 2014). More strikingly, however, a constitutive DELLA protein that is insensitive to GA is able to overcome the mycorrhizal impairment of two mutants of the common symbiotic signaling cascade (Pimprikar *et al.*, 2016). This cascade links fungal perception to the activation of the first mycorrhiza-specific transcription factor, RAM1, which is sufficient to restore arbuscule development even in the presence of GA (Pimprikar *et al.*, 2016). RAM1 activates a downstream series of essential components required for the PAM development and for the nutrient exchange through that interface (Luginbuehl & Oldroyd, 2017).

Accommodation of arbuscules in inner cortical cells also impacts on cortical root cell development. A few reports on morphometric analyses showed that fungal colonization induced cellular changes that affected root diameter, mitotic index, cell size and cell wall thickness (Berta *et al.*, 1995; Balestrini *et al.*, 2005; Russo *et al.*, 2019a). However, the molecular mechanisms behind these changes were unknown. In a previous study, we were able to demonstrate that AM symbiosis induces the expression of three GRAS transcription factors (MIGs) and that one of them, MIG1, is specifically induced in arbuscule-containing cells where it acts as a key regulator of cortical cell expansion (Heck *et al.*, 2016). MIG1 ectopic expression also increased the number of cortical cell layers and, as a result, the root diameter. All MIG1 responses are counteracted by GA, and its silencing impairs arbuscule development. Expression of a dominant active DELLA rescues this phenotype, suggesting that MIG1 and DELLA act in concert to promote the radial cell expansion required for arbuscule development (Heck *et al.*, 2016). Here we show that this process is fine-tuned by the concomitant activity of the two MIG1 paralogues, MIG2 and MIG3, and the GRAS transcription factor SCL3. MIG3 and SCL3 act in concert with the central regulator DELLA in arbuscule-containing cells to restrain cell expansion, thus counteracting the positive expansion effects of the complexes of MIG1 and MIG2 with DELLA to allow the accommodation of the developing arbuscule.

Materials and Methods

Biological material, transformation and plant growth conditions

Medicago truncatula Gaertn. cv Jemalong A17 or *M. truncatula* R108 double mutant *della1/della2* plants (Floss *et al.*, 2013) were grown in growth chambers at 25°C with a 16 h : 8 h, light : dark photoperiod. *Medicago truncatula* plants were transformed using *Agrobacterium rhizogenes* strain ARqual (Quandt *et al.*, 1993) according to a previously described method (Boisson-Dernier *et al.*, 2001). Transformed plants were cultivated for 5 wk on Fahraeus plates. Successfully transformed roots were visually selected based on the constitutive expression of the inserted DsRED1 cassette and nontransgenic roots were excised. Composite plants (transformed roots and wild-type shoots) were then grown in 50 ml Falcon tubes (Thermo Fischer Scientific GmbH, Karlsruhe, Germany) with a 5 : 1, sand : gravel mixture, and were watered with half strength Long Ashton nutrient solution (20 µM Pi, 4mM N) twice per wk (5 ml), for 5 wk.

All experiments were carried out with the ecotype A17, except those shown in Fig. 4 and Supporting Information Fig. S6, where the genetic background *della1/della2* in the ecotype R108 was used (Floss *et al.*, 2013).

Plant size measurements for all experiments are given in Table S1.

Nicotiana benthamiana was used for transient expression of proteins and was grown on soil at 22°C, with 16 h : 8 h, light : dark photoperiod.

Rhizophagus irregularis DAOM 197198 (Schenck & Smith, 1982) was cultivated in monoaxenic cultures as described previously (Kuhn *et al.*, 2010). *Medicago truncatula* plants were inoculated with *R. irregularis* using inoculum from colonized carrot roots from a monoxenic culture (1/2 plate inoculum for 50 ml substrate). Noncolonized plants did not receive any additives. Plants were grown for 5 wk in 50 ml Falcon tubes covered with aluminium foil under the conditions described in the first paragraph of this section. The number of analyzed biological replicates for each experiment are shown in the corresponding figure legend of each figure.

Generation of constructs used in this study

For promoter–reporter assays, two fragments (1 kb for *MIG2* and 2 kb for *MIG3* and for *SCL3*) upstream of the start codon ATG were cloned into the binary Gateway destination vector pPGFPUS-RedRoot (Kuhn *et al.*, 2010). For overexpression analyses in *M. truncatula* roots, the coding sequences of *MIG2* (Medtr2g034260), *MIG3* (MTR_2g034250) and *SCL3* (Medtr5g009080) were amplified from cDNA and cloned into the destination vector 2xP35S-pKGW-RedRoot (Heck *et al.*, 2016). For simultaneous overexpression analyses in *M. truncatula* roots, the coding sequence of *MIG3* together with the P35S promoter and a terminator sequence was amplified from the MtMIG3OE_2xP35SpKGW-RR destination vector. The amplified fragments contain the *SpeI* and *AsiI* restriction sites. Destination vectors with the 2xP35S promoter and the RedRoot cassette

containing either *MIG1* (Heck *et al.*, 2016) or *MIG2*, constructed as described above, were digested with *SpeI* and *Ascl* to clone *MIG3*. Silencing of *SCL3* was carried out using the vector pRED-RNAi with the *PT4* promoter from *M. truncatula* (Devers *et al.*, 2013). A 216 bp RNAi construct covering the region from +29 to +229 with respect to the ATG was amplified from cDNA and cloned in sense (*BamHI* and *BsrGI*) and antisense (*BspEI* and *HindIII*) directions, with a spacer sequence forming a hairpin structure. The sequence of the *SCL3* RNAi construct is as follows:

```
ttcatcagtaactgtttccactctacagtattttccatgatgtcagtttcacctaacatagga  
ggaataggatcaccttatccatggcttagtagaga  
attgaaatcggaggaaaggggtttgtattgtatccattgttaactcactgtgcaaacat  
gtagcttctgtagtcttgaagtcaaacacaacactt
```

For interaction assays using bimolecular fluorescence complementation (BiFC) N-terminal fusions of the *SCL3* ORF to the N- or C-terminal YFP-halves were cloned into the binary vectors P35S-pSPYNE-GW and P35S-pSPYCE-GW (Walter *et al.*, 2004). Further constructs used in this study are described in a previous article (Heck *et al.*, 2016). All primers used for cloning of the constructs described above are listed in Table S2.

For co-immunoprecipitation (CoIP), *MIG3* was N-terminally tagged with green fluorescent protein (GFP), while *SCL3* was C-terminally tagged with the Myc epitope using the binary vectors pK7WGF2 (P35S-eGFP-attR1-CmR-ccdB-attR2) and pGWB17 (P35S-attR1-CmR-ccdB-attR2-4xMyc) (Nakagawa *et al.*, 2007). Primers used for cloning are listed in Table S2.

Histochemical β -glucuronidase (GUS) analysis

Promoter-reporter studies were carried out using mycorrhizal and control composite plants harvested 5 wpi (weeks post-inoculation). Roots were incubated in fixation solution (50 mM NaH_2PO_4 , 50 mM Na_2HPO_4 , 1 mM EDTA, 37% formaldehyde) for 30 min. Incubation in staining solution (50 mM NaH_2PO_4 , 50 mM Na_2HPO_4 , 1 mM EDTA, 1 mM X-GlcA (Apollo Scientific Ltd, Bredbury, UK; stock solution 0.1 M in DMF)) was carried out overnight at 37°C. The staining was fixed in 50% EtOH before counterstaining fungal structures with wheat germ agglutinin-fluorescein isothiocyanate conjugate (WGA-FITC) as described by Rech *et al.* (2013).

Gene expression analysis

Total RNA extraction, cDNA synthesis and quantitative real-time polymerase chain reaction (qRT-PCR) were carried out as described in (Kuhn *et al.*, 2010), with minor changes: 1 μl cDNA (1 : 5) was used per well as template. The PCR protocol selected was as follows: 5 min at 95°C, 15 s at 95°C, 15 s at 56°C, 30 s at 72°C (40 cycles). Transcript levels of genes were determined in at least four biological replicates, with at least three technical replicates per reaction. Transcript levels of the translation elongation factor 1-alpha of *M. truncatula* (*MtTEF1a*, Medtr6g021800) were used for normalization (Wulf *et al.*, 2003). All primers are listed in Table S2.

Bimolecular fluorescence complementation

For BiFC assays, 3–4-wk-old leaves of *N. benthamiana* plants were infiltrated with *Agrobacterium tumefaciens* GV1301 transformed with P35S-pSPYNE-GW and/or P35S-pSPYCE-GW expressing the genes of interest fused to the YFP-halves or as empty vectors (EV). The p19 protein of tomato bushy stunt virus was used to suppress gene silencing in co-transformation (Voinnet *et al.*, 2003). Cells were kept overnight in infiltration media (2% sucrose solution 10 mM MgCl_2 , 10 mM MES, 150 μM acetosyringone in dimethyl sulfoxide (DMSO)), with an OD_{600} of 0.8–1.0 at room temperature before co-infiltration with a ratio of 1 : 1 : 1. After infiltration, plants were kept at room temperature in a low illuminated place. Images were taken 2 d after infiltration.

Co-immunoprecipitation assays and Western blots

For co-immunoprecipitation assays, appropriate constructs were transiently expressed in *N. benthamiana* as described above. Per assay, a minimum of three leaves from two plants were infiltrated with the *A. tumefaciens* mixture using a needleless syringe. Three days after infiltration, four leaf discs per sample were harvested. Leaf tissue was ground in liquid nitrogen in a Retsch mill (Resch GmbH, Edingen-Neckarhausen, Germany) and 550 μl extraction buffer (0.5% (w/v) polyvinylpyrrolidone, 10% Tween20, 100 mM PMSF, 5% NP40 and a protease inhibitor PIC tablet (cat. no. 04693159001; Roche Diagnostic GmbH, Freiburg, Germany)) was added per sample. Samples were incubated on ice for 15 min and sonicated (5 min, 15 s on, 30 s off; amplitude 40%). Supernatant was filtered through an 80 μm nylon mesh (Sigma-Aldrich); 30 μl were taken for the input sample and the rest of the filtered extract was added to 50 μl equilibrated GFP-binding affinity magnetic beads (GFP-Trap magnetic GFP beads; ChromoTek GmbH, Planegg, Germany). Samples were incubated on a test tube rotator for 2 h at 4°C. GFP-Trap magnetic GFP beads were magnetically separated and washed at least three times with 500 μl washing buffer (0.5% (w/v) polyvinylpyrrolidone, 10% Tween20, 100 mM phenylmethylsulfonyl fluoride (PMSF) and a PIC tablet (Roche Diagnostic GmbH)). Proteins were eluted by adding 90 μl 2 \times Laemmli buffer (containing 10% β -mercaptoethanol) followed by incubation for 10 min at 95°C. Immunoprecipitated proteins were dissolved in 40 μl Laemmli buffer and loaded, together with input samples (10 μl Laemmli buffer and 30 μl of protein extract), onto an 8% (w/v) sodium dodecyl-sulfate (SDS)-polyacrylamide gel. Proteins were then transferred to a 0.2 μm nitrocellulose membrane (Amersham Protran membranes, Merck KGaA, Darmstadt, Germany) for 2 h in Dunn carbonate buffer at 4°C while steering. Membranes were first stained with Ponceau to evaluate protein transfer. After washing with 0.1 M NaOH, the membranes were blocked in 5% instant nonfat dry milk (w/v, blotting grade milk powder; Carl Roth GmbH, Karlsruhe, Germany) in 1 \times PBS for 1 h. After washing with 0.1 M NaOH, membranes were blocked in 5% instant nonfat dry milk (w/v, blotting-grade milk powder, Carl Roth GmbH) in 1 \times PBS for 1 h. Afterwards, membranes were incubated with the primary antibody (anti-GFP (G1544) or anti-Myc

(M5546; Sigma-Aldrich) in 2.5% instant nonfat dry milk (w/v) in 1× PBST (1× PBS, 0.05% Tween20) at 4°C overnight (GFP, 1 : 4000; Myc, 1 : 500). Membranes were then washed three times for 10 min with PBST and incubated with peroxidase-conjugated secondary antibody (anti-mouse (A2304) or anti-rabbit (A0545); Promega) in 2.5% instant nonfat dry milk (w/v) in 1× PBST for 1 h at room temperature (GFP, anti-rabbit (1 : 4000); Myc, anti-mouse (1 : 2000)). Membranes were then washed three times for 10 min with PBST and incubated with a luminescent solution (1 ml solution A: 50 ml 0.1 M Tris-HCl (pH 8.6), 12.5 mg Lumi-nol (cat. no. A4685; Sigma-Aldrich); 100 µl solution B: 11 mg p-hydroxycoumarin acid (cat. no. C9008; Sigma-Aldrich) in 10 ml DMSO; and 0.5 µl 35% H₂O₂) and exposed to an X-ray film (FujiFilm, Düsseldorf, Germany). SCL3-Myc was detected with a size of 60.35 kDa and MIG3-GFP with 94.09 kDa.

Phenotypical analysis and quantification of mycorrhizal levels

For phenotypical analysis and quantification of mycorrhizal roots, fungal structures were stained with WGA-FITC as described by Rech *et al.* (2013). Quantification of mycorrhizal structures was carried out according to the method described by Trouvelot *et al.* (1986), using a fluorescence confocal microscope (see next paragraph). The following parameters were analyzed: F%, which represents the frequency of mycorrhizal colonization in the root system; M%, the intensity of colonization; A%, the abundance of arbuscules; and I%, the abundance of intraradical hyphae.

For morphometrical analyses of cell or arbuscule length and width, as well as of root diameter, images were taken randomly from actively growing secondary roots emerging from primary transformed roots. Analyzed roots were always of the same age and were compared to their corresponding empty vectors. Cell measurements were carried out on lateral roots in sections comprised between 2 cm of the lateral root emergence and 2 cm above the tip, avoiding meristematic regions as well as areas of lateral root emergence. Areas containing arbuscules for mycorrhizal plants and corresponding areas in nonmycorrhizal plants were selected. The number of cortical cell layers was counted independently on both sides of the central cylinder, in each biological replicate. Cell size was measured in radial and longitudinal directions, always in inner layers of the cortex, and only in cells in which all borders were in focus. The exact numbers of biological replicates, roots, and cells are indicated in each figure legend (Figs 2–4 and 6). Arbuscule size was analyzed in areas of actively developing arbuscules for each infection unit analyzed. The analyzed roots were always of the same age and were compared to the corresponding control roots (transformed with an EV). Measurements were carried out using the Fiji software package (<http://fiji.sc/Fiji>).

For root sections, secondary roots were fixed in 4% paraformaldehyde and dehydrated in an EtOH series. Root fragments were embedded in Paraplast Plus Sigma-Aldrich (Merck KGaA, Darmstadt, Germany) and sectioned using a mechanical microtome (15 µm and 20 µm cuts). The root sections were stained with 0.1% (w/v) Toluidin Blue O (Carl-Roth GmbH) and mounted in Entellan new (Sigma-Aldrich).

Confocal microscopy and image processing

Microscopy analyses were carried out using a confocal microscope (TCS SP5 (DM5000); Leica Biosystems GmbH, Nussloch, Germany) with conventional photomultiplier tube (PMT) detectors and a Leica DFC295 color camera. The WGA-FITC stained roots and eYFP in BiFC analyses were both excited with an argon laser at 488 nm and 514 nm. Emission was detected from 505–525 nm (fluorescein) and from 530–605 nm (eYFP). Images were processed using the Fiji software package.

In silico analysis and secondary structure prediction

In silico expression data were obtained from the *M. truncatula* gene expression atlas (<http://mtgea.noble.org/v3/>) (Benedito *et al.*, 2008).

Amino acid alignments were conducted with CLUSTALW and CLUSTALO using the neighbor-joining method in MEGA7 (<http://www.megasoftware.net/>) (Kumar *et al.*, 2016), a bootstrap value of 1000 (percent value is labelled at each node), p-distance, and pairwise gap deletion parameters are shown in the phylogenetic tree. GRAS protein sequences from Arabidopsis and *M. truncatula* were retrieved from the NCBI databases (<https://www.ncbi.nlm.nih.gov/> and <http://jcv.org/medicago/>).

Quantification and statistical analysis

Results regarding root diameter and numbers of cortical cell layers are represented as bar charts showing the mean and SD. Cell width and cell length, as well as gene expression, are shown as box-and-whisker plots, representing the first, second (median) and third quartiles, and the highest and lowest data points within a 1.5-interquartile range (IQR). Outliers are represented by blue circles. The Kolmogorov–Smirnov test was used to test for a normal distribution. The two tailed Student's *t*-test (with two degrees of freedom) was used for pairwise comparison of qRT-PCR data, arbuscule size and quantification. The two tailed Mann–Whitney *U*-test was used for pairwise comparison of morphometrical analysis of roots and cells (<https://www.socscistatistics.com/tests/mannwhitney/>). For comparisons involving more than two groups and showing no normal distribution, the significance was calculated using the Kruskal–Wallis test and the *post-hoc* Tukey–Kramer test (<https://astatsa.com>). Significant differences with *P* < 0.05 are shown in the corresponding figures with different letters. The exact *P*-values for each experiment described in this paper are given in Table S3. The exact numbers (*n*) of biological and technical replicates, as well as the statistical tests employed are indicated in each figure legend.

Results

The MIG1 paralogues, MIG2 and MIG3, are induced in arbuscule-containing cells

MIG1 has two paralogues, *MIG2* and *MIG3*, and all three are located in tandem on chromosome two (Heck *et al.*, 2016). The expression of all *MIG* genes increases during mycorrhiza

symbiosis and in response to a spore extract of the AM fungus *R irregularis* (Heck *et al.*, 2016). However, only *MIG2* and *MIG3* basal expression was clearly observed under nonsymbiotic conditions. Given the high level of homology among the three proteins (between 79% and 82% of identity), the fact that *MIG1* is more specifically expressed during symbiosis suggests a neofunctionalization to control specific tasks in colonized cortical cells. In order to test this hypothesis and to investigate the role of *MIG2* and *MIG3*, we first compared transcript accumulation of all *MIG* genes using GUS promoter–reporter analyses. Because the sequence of the promoter region of *MIG2* deposited in NCBI was incorrect, we amplified by chromosome walking a 1-kb region upstream of the ATG (MZ673802.1) and used it for promoter GUS assays (Fig. S2). *MIG2* and *MIG3* were expressed ubiquitously and abundantly in roots under nonmycorrhizal conditions. By contrast, *MIG1* under those conditions is only expressed in the central cylinder (Fig. 1a). However, in *R. irregularis* colonized roots, *MIG2* and *MIG3* expression is notably

enhanced in cortical cells harbouring arbuscules, while *MIG1* expression is confined exclusively to the cortical area containing arbuscules (Figs 1a, S1). These data are supported by transcriptomic data from microdissected arbuscules (Zeng *et al.*, 2018) deposited in the *M. truncatula* gene atlas (dataset 20210401; <https://medicago.toulouse.inrae.fr/MtExpress>).

The presence of the conserved ‘CTTC’ motif in the promoter of the *MIG* genes is consistent with their induction in cells harbouring arbuscules. The CTTC motif has been identified in the promoter of several genes expressed in arbuscule-containing cells and has been shown to be necessary, but not sufficient, for the induction of the symbiotic phosphate transporter *PT4* (Chen *et al.*, 2011; Lota *et al.*, 2013; Krajinski *et al.*, 2014). Surprisingly, in contrast to *MIG1* and *MIG2*, *MIG3* does not contain any of these motifs in close proximity to the ATG; instead, they are located further upstream (Figs 1b, S2). Furthermore, only *MIG1* and *MIG3* promoters contain a P1BS motif for activation by the PHR1 transcription factor upon phosphate

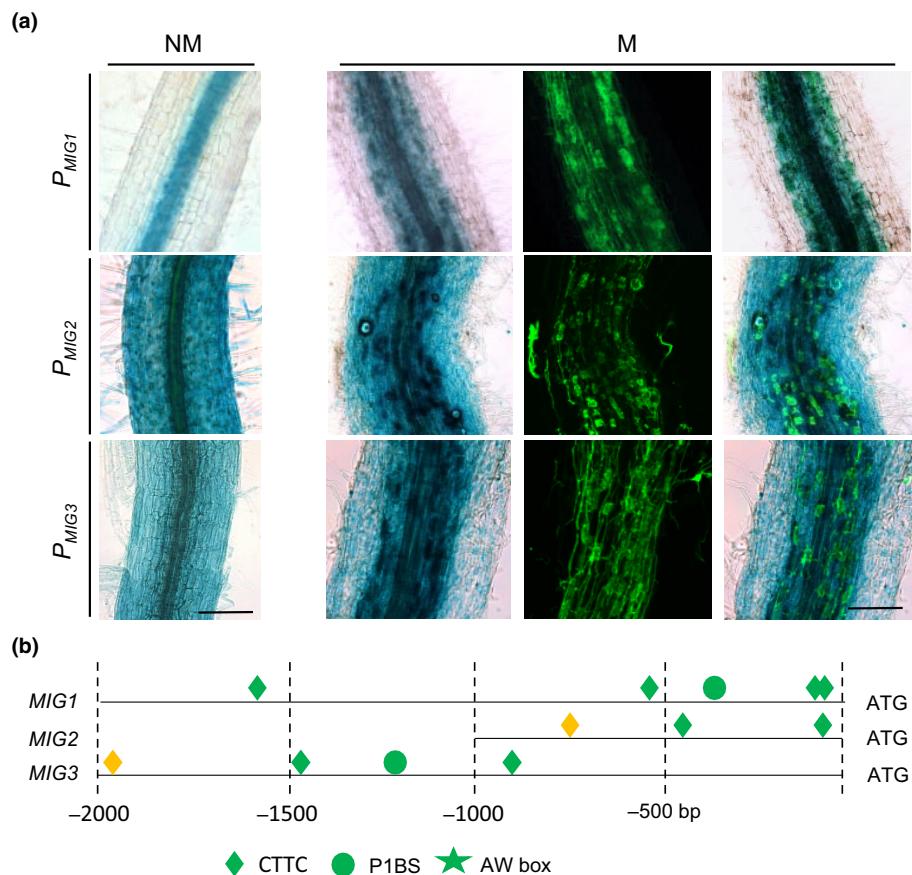


Fig. 1 *MIG2* and *MIG3*, paralogues of *MIG1*, are also induced in arbuscule-containing cells. (a) β -glucuronidase (GUS) promoter–reporter analyses for *MIG* genes were carried out in *Medicago truncatula* transformed roots. Nonmycorrhizal (NM) roots expressing P_{MIG1} :GUS show activity only in the central cylinder, in contrast to roots transformed with P_{MIG2} :GUS or P_{MIG3} :GUS, which show activity throughout the whole root. Mycorrhizal (M) roots expressing the 2 kb P_{MIG1} show activity exclusively in arbusculated cells, while the 1 kb P_{MIG2} or the 2 kb P_{MIG3} are induced not only in arbuscule containing cells, but also in all other root cells. Bars, 100 μ m. In mycorrhizal roots (M) panels show: Left: brightfield; middle: wheat germ agglutinin–fluorescein isothiocyanate conjugate (WGA-FITC) to visualize fungal tissue; right: overlay. (b) *In silico* analysis of *MIG* promoter regions upstream from the ATG. The *cis*-regulatory element CTTC, characteristic of genes induced in arbuscules, with a maximum of a single base-pair exchange with respect to the consensus sequence (TCTTGTC) is represented by a diamond. The P1BS motif, for binding of the phosphate starvation regulator PHR1, is represented by a circle. The AW box motif for binding the CBX1 transcription factor with the consensus sequence (CnTnG(n)₇CG) is represented by a star. Motifs on the + strand are green, motifs on the – strand are orange.

starvation (Rubio *et al.*, 2001). The P1BS motif has been identified in combination with the CTTC motif in several arbuscule-induced genes (Lota *et al.*, 2013; Krajinski *et al.*, 2014). Surprisingly, we could not identify an AW box in the promoter of the MIG genes. The AW box has been shown to be bound by the transcription factor WRI5a in *M. truncatula* and to induce many of the arbuscule-induced genes (Jiang *et al.*, 2018). Furthermore, LjCBX1 was also shown to bind the AW box (Xue *et al.*, 2018). LjCBX1 ectopic expression is sufficient to induce key markers of the symbiosis, even in suspension cells of the nonhost *Arabidopsis*. Interestingly, a genome-wide analysis of CBX1 targets in *Lotus japonicus* identified, among others, the orthologue of *MIG1* and two other *MIG1*-like genes (Xue *et al.*, 2018). This suggests that CBX1 could be the mycorrhizal transcription factor inducing *MIG* genes in arbuscule-containing cells. However, the role of these *cis*-regulatory elements requires further experimental validation.

Overexpression of *MIG2*, but not of *MIG3*, phenocopies the root cortical cell developmental changes induced by *MIG1*

The high sequence similarity between the three *MIG* paralogues suggested that their functions could be related or even identical. However, silencing of individual genes proved difficult due to their homology (Heck *et al.*, 2016; N. Requena & C. Seemann, unpublished data) and thus we investigated the individual functions of *MIG2* and *MIG3* by overexpression analysis. Surprisingly, morphometric analysis of *M. truncatula* roots ectopically expressing *MIG2* or *MIG3* revealed that there were important differences. Thus, under nonmycorrhizal conditions, overexpression of *MIG2* induced many alterations in the root cortex morphology (Figs 2a, S3). Root diameter was enlarged, consistent with an increase in the number of cortical cell layers, as well as with an increase in the cell width; however, cortical cell length was also significantly increased (Fig. 2b). This indicates that *MIG2* fully phenocopies the effects observed when ectopically expressing *MIG1* under nonmycorrhizal conditions (Heck *et al.*, 2016). By contrast, overexpression of *MIG3* resulted in a reduced root diameter that paralleled a decrease in cortical cell width and length, although the number of cortical cell layers remained unaffected (Fig. 2a,c). This is remarkable, given that all three proteins share such a high degree of conservation. However, this conservation is reduced when considering only the amino terminus, which is the domain that delimits the GRAS transcription factors that belong to the *MIG* clade (Heck *et al.*, 2016). This domain is more highly conserved between *MIG1* and *MIG2* (73% identity) than between either *MIG2* and *MIG3*, or *MIG1* and *MIG3* (between 55% and 64%). The homology to *MIG3* is particularly reduced in two amino acid stretches located before the three conserved alpha helices where the putative DNA binding domains were identified (Fig. S4). Altogether, these results suggest that the mechanisms by which *MIG1* and *MIG2* induce cell expansion and cortical cell divisions are differently regulated by *MIG3*.

Fungal root colonization increased cortical cell width, in agreement with our previous observations (Heck *et al.*, 2016).

But in addition, we also report here that symbiosis augments the number of cortical cell layers, something that went unnoticed previously, further contributing to the increase in root diameter (Fig. 2b,c). By contrast, the cortical cell length of cells containing arbuscules was inconsistently modified (Fig. 2b,c). Although we do not have a clear explanation for this effect, the anticlinal cell divisions observed sparsely in the inner cortical layer of AM colonized plants (Russo *et al.*, 2019a,b) might partly account for these variations. In support of this, expression of the cyclin F-box protein (*CYC1*) is induced by *MIG3*, especially under mycorrhizal conditions (Fig. S5). Interestingly, ectopic expression of *MIG2* or *MIG3* significantly and inversely altered the effects on root cortex morphology exerted by *R. irregularis*. Thus, in mycorrhizal plants, *MIG2* ectopic expression further enhanced root diameter through an increase in the number of cortical cell layers, but cell width was not further increased (Fig. 2b). By contrast, overexpression of *MIG3* reduced cell width (and length) thus decreasing the root diameter without affecting the number of cortical cell layers (Fig. 2c). These and our previous results confirm that cortical cell expansion is regulated by *MIG* transcription factors during symbiosis. *MIG1* and *MIG2* act as positive regulators, while *MIG3* somewhat restrains cortical cell expansion.

Ectopic expression of *MIG3*, but not of *MIG2*, negatively impacts arbuscule development

To address the question of how the changes in cell morphology imposed by *MIG2* and *MIG3* ectopic expression would affect the development of the fungus in the cortex, the symbiotic fungal structures were analysed. In agreement with the results in the above section, *MIG2* overexpression did not cause any significant alteration of the overall mycorrhizal colonization (Fig. S3), nor did it modify the expression of the fungal gene *RiTEF* or the plant phosphate transporter *MtPT4*, an arbuscule-specific marker (Fig. 3b). It also did not have a major impact on the arbuscule size or morphology, although arbuscule width was somewhat increased (Figs 3a,b, S3). By contrast, overexpression of *MIG3* negatively impacted on symbiosis progression and overall colonization, resulting in a lower fungal density for all parameters analyzed and a reduced *RiTEF* expression (Fig. S3). Also, *MtPT4* levels were significantly reduced (Fig. 3c), correlating with a lower number of arbuscules. But most remarkably, the average size of arbuscules was considerably reduced in those plants, corresponding to the reduced size of cortical cells (Figs 3a,c, S3). These results indicate that although the expression of all three *MIG* genes is induced in colonized roots, in contrast to *MIG1* and *MIG2*, *MIG3* negatively affects cell size, impacting arbuscule development either directly or indirectly.

We hypothesize that during symbiosis, *MIG3* may counteract the expanding effects of *MIG1* and *MIG2* on cortical cell morphology to properly regulate arbuscule development. In order to test whether *MIG3* could reverse the effects mediated by *MIG1* and *MIG2*, their corresponding genes were overexpressed simultaneously. Morphometric analyses of roots showed that the promoting effects mediated by *MIG1* or *MIG2* on

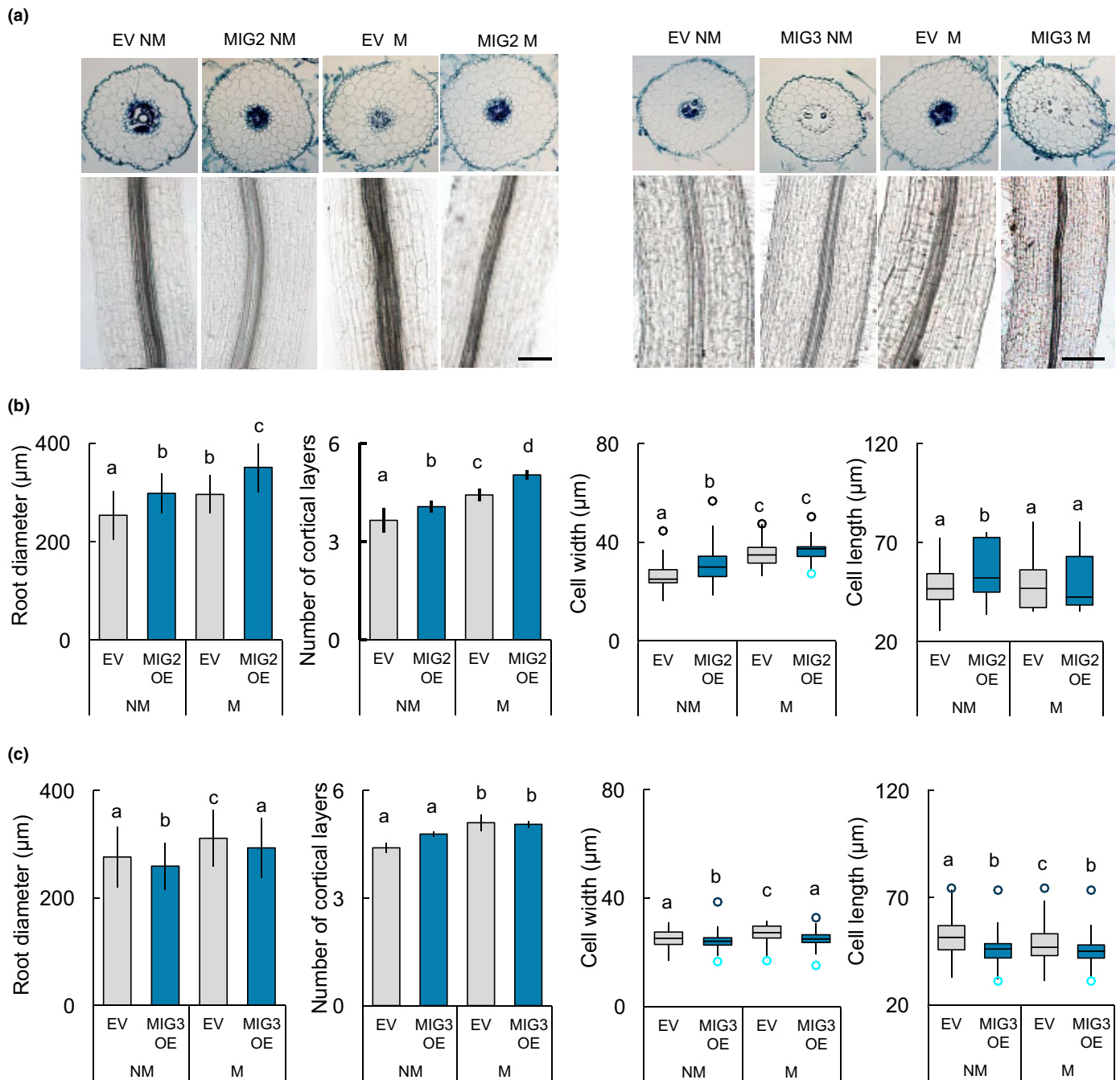


Fig. 2 Overexpression of *MIG2*, but not of *MIG3*, phenocopies the root cortical cell developmental changes induced by *MIG1*. (a) Radial and longitudinal root sections of nonmycorrhizal and mycorrhizal roots expressing $2xP_{35S}::MIG2$, $2xP_{35S}::MIG3$ or an empty vector (EV) are shown. Bars, 100 μm. (b, c) Morphometric analyses (root diameter and number of cortical cell layers, as well as cortical cell width and length) were carried out using the Fiji software package. At least five biological replicates per treatment were used, with n (roots) ≥ 65 per treatment, n (cells) ≥ 195 for *MIG2*, and n (cells) = 450 for *MIG3*. Data represent mean values (root diameter, number of cortical cell layers) \pm SD. Box-and-whisker plots show the first, second and third quartiles, and the highest and lowest data points within a 1.5-interquartile range (IQR) are shown. Outliers are represented by blue circles. The Kolmogorov–Smirnov test was used to test for a normal distribution. Significance was calculated using the Kruskal–Wallis test and the Tukey–Kramer *post-hoc* test. Different lowercase letters indicate significant difference ($P < 0.05$).

cortical cell expansion were abolished by co-expression with *MIG3* in nonmycorrhizal conditions, indicating that even without the presence of the fungus, *MIG3* is dominant over *MIG1* and *MIG2* (Figs 3d–f, S3). Furthermore, under mycorrhizal conditions, simultaneous expression of *MIG3* and *MIG1* or

MIG2 also reduced cell expansion in both cases, with a parallel reduction in arbuscule size (Figs 3d–f, S3). Taken together, these results suggest that the fine-tuning of cell size during arbuscule development is achieved by an interplay between all three *MIG* proteins.

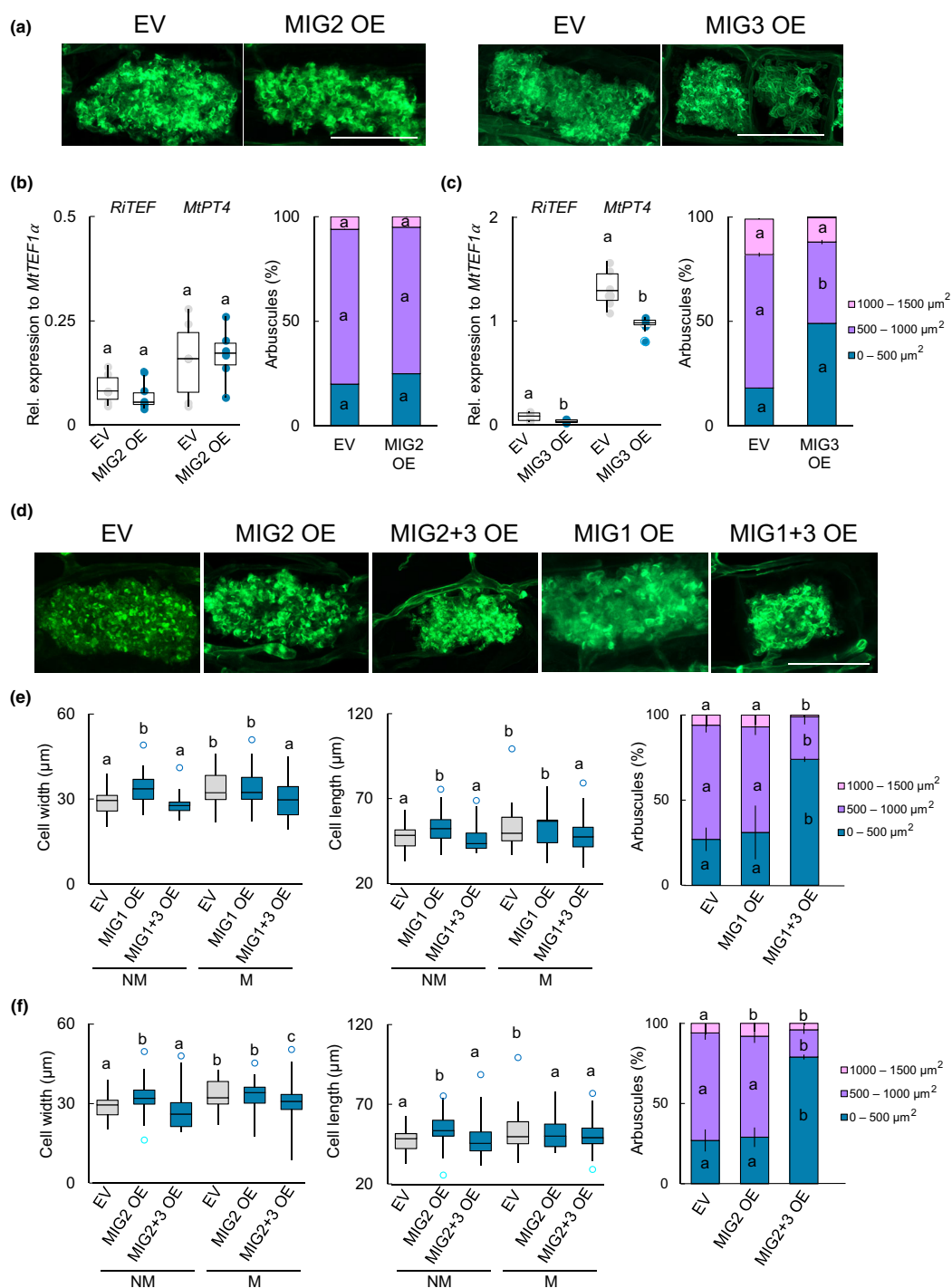


Fig. 3 Ectopic expression of *MIG3*, but not of *MIG2*, negatively impacts on arbuscule development. (a, d) Representative examples of arbuscules in plants ectopically expressing either *MIG1*, *MIG2*, *MIG3*, *MIG1+MIG3* or *MIG2+MIG3* and their corresponding empty vector (EV) are shown. Bars, 25 μm . (b, c) Transcript accumulation of *RiTEF* and *MtPT4* was analyzed by quantitative real-time polymerase chain reaction (qRT-PCR) relative to the housekeeping gene *MtTEF1α* in *MIG2* (b) or in *MIG3* (c) expressing plants compared to EV plants. (b, c) Arbuscule area (length \times width) distribution was analyzed in *MIG2*- or *MIG3*- as well as in EV-expressing plants using the Fiji software package. The data regarding Arbuscule area were grouped into three categories (0–500 μm^2 , 500–1000 μm^2 , 1000–1500 μm^2), and the percentage of arbuscules belonging to each category is shown as a bar chart. Per biological replicate ($n \geq 5$), we measured 125 arbuscules ($n = 125$). Data represent mean \pm SD. Significance was calculated using the two-tailed Student's *t*-test. Significance is given at $P < 0.05$ and is indicated by different lowercase letters. (e, f) Morphometric analyses (cortical cell width and length) were conducted in *MIG1*-, *MIG2*-, *MIG1+3*-, *MIG2+3*- and EV-expressing plants using the Fiji software package, both in mycorrhizal (M) and nonmycorrhizal (NM) conditions. At least five biological replicates per treatment were used, with n (roots) ≥ 65 per treatment and n (cells) ≥ 300 . Similar to (b, c) arbuscule area was analyzed for $n = 125$ arbuscules. For all box-and-whisker plots in this figure, the first, second and third quartiles, and the highest and lowest data points within a 1.5-interquartile range (IQR) are shown. Outliers are represented by blue circles. The Kolmogorov–Smirnov test was used to test for a normal distribution. Significance was calculated using the Kruskal–Wallis test and the Tukey–Kramer *post-hoc* test. Different letters indicate significant difference ($P < 0.05$).

MIG proteins require DELLA to control cortical cell width

In order to investigate how MIG proteins could exert their control over cortical cell and arbuscule size, we analyzed their interactions with other GRAS transcription factors using BiFC. Similar to MIG1, which neither interacts with itself nor with MIG2 or MIG3 (Heck *et al.*, 2016), MIG2 and MIG3 are unable to form homo- or heterodimers with each other (Fig. S6). Because we had shown before that MIG1 is able to interact with DELLA1, and that a constitutive active DELLA protein rescues the arbuscule phenotype observed in *MIG1* silenced roots (Heck *et al.*, 2016), we next analyzed the interaction of MIG proteins with all *M. truncatula* DELLA proteins. All MIG proteins were able to interact with DELLA1, but in addition MIG2 and MIG3 showed interaction with DELLA2 and DELLA3 (Figs 4a, S6). Although these results require further validation by other protein–protein interaction methods, they suggest that the interaction of MIG proteins with DELLA proteins could be a central element in the control of cortical cell width, not only in arbuscule-containing cells, but also in a nonsymbiotic context, as MIG2 and MIG3 are ubiquitously expressed throughout the cortex under those conditions.

To determine whether DELLA is required for the promoting or restraining effects of MIG1 or MIG3, respectively, we expressed these proteins in the *della1/della2* genetic background (Fig. S6) and conducted morphometric analyses. We showed previously (Heck *et al.*, (2016)) that the *della1/della2* mutant in the ecotype R108 has a reduced diameter as a result of a reduced number of cortical cell layers, consistent with the expectation that increased GA signaling causes the slender phenotype (Floss *et al.*, 2013). The results of the overexpression of the MIG genes in this genetic background indicated that DELLA1/2 are necessary for the increase in cell width and root diameter exerted by MIG1 but, surprisingly, not for the increase in the number of cortical cell layers (Fig. 4b). This was unexpected, because a constitutive active DELLA is itself able to promote periclinal cortical cell divisions in *M. truncatula* (Heck *et al.*, 2016). More interestingly, in the *della1/della2* genetic context, MIG3 no longer acted as a negative regulator and promoted root diameter by increasing cell width, despite a reduction in the number of cortical cell layers (Fig. 4c). These contrasting phenotypes could perhaps be explained in light of the fact that DELLA3 is still present in this mutant background. However, we only observed interaction between MIG3 and DELLA3, but not between MIG1 and DELLA3 (Figs 4a, S6 and Heck *et al.*, 2016). Altogether, these results imply that both MIG1 and MIG3 act in concert with DELLAs to control root cortex development, by activating or repressing downstream regulators of cortical cell expansion.

SCL3 is induced in arbuscule-containing cells and interacts with MIG3

In order to investigate which other regulators could be participating in adjusting cortical cell size and arbuscule development in response to MIG proteins, we turned our attention to the Scarecrow-like (SCL) transcription factors. They have been

shown to be crucial factors in the determination of post-embryonic cortex formation, and to regulate root cortex morphology (Choi & Lim, 2016). Several SCL genes have been shown to be transcriptionally regulated during mycorrhiza symbiosis (Gomez *et al.*, 2009; Hogeekamp *et al.*, 2011; Bravo *et al.*, 2016; Heck *et al.*, 2016; Ho-Plagaro *et al.*, 2019). But most interestingly, one of these genes, which we name *SCL3* here (Medtr5g009080), was shown to be induced in seedlings of *M. truncatula* in response to the same *R. irregularis* spore extract that also induced the MIG genes (Heck *et al.*, 2016). Therefore, we next investigated the role of SCL3 during symbiosis and in relation to the function of MIG proteins.

Using the GUS promoter–reporter assay, we were able to show that *SCL3* expression in *M. truncatula* roots is restricted to the inner cortex but is induced in arbuscule-containing cells during symbiosis, in agreement with the presence of the CTTC motif in its promoter (Figs 5a, S7), and in agreement with transcriptomic data of microdissected arbuscules (Zeng *et al.*, 2018). This is also true in tomato, where *SIGRAS18* was also induced in arbuscule-containing cells (Ho-Plagaro *et al.*, 2019). We next analyzed *SCL3* expression in roots ectopically expressing either *MIG1* or *MIG3*. Interestingly, while ectopic expression of *MIG1* or a dominant DELLA ($\Delta 18DELLA1$) did not significantly change *SCL3* accumulation, their simultaneous expression reduced the *SCL3* transcript under nonmycorrhizal conditions (Fig. 5b). By contrast, overexpression of *MIG3* induced *SCL3* but only under mycorrhizal conditions (Fig. 5b). These results suggest an interplay between the MIG transcription factors, the DELLA proteins and SCL3. This hypothesis is supported by the interaction among these proteins shown in BiFC assays (Fig. 5c). Thus, SCL3 interacts directly with all three DELLA proteins, in a similar manner as AtSCL3 interacts with DELLA in Arabidopsis (Zhang *et al.*, 2011). But most interestingly, SCL3 also interacts with MIG3 but not with MIG1 or MIG2 (Figs 5c,d, S7). Therefore, we speculated that SCL3 could be contributing, together with the MIG and the DELLA proteins, to the regulation of cortical cell expansion in arbuscule-containing cells.

SCL3 is a negative regulator of cortical radial cell expansion during AM symbiosis

To test this hypothesis, *SCL3* expression was deregulated to investigate root cortex development. *SCL3* overexpression provoked similar effects to MIG3. Hence, it reduced cell width and cell length, therefore diminishing the root diameter, but it did not modify the number of cortical cell layers (Figs 6a, S8). However, this effect was only observed under mycorrhizal conditions, consistent with the fact that MIG3 only induces expression of *SCL3* during symbiosis (Fig. 5b) and indicating the requirement of an additional unknown transcription factor only induced in symbiosis. Because ectopic expression of *SCL3* only showed a root cortex phenotype in symbiosis, we decided to silence its expression using an arbuscule-specific promoter as we had done previously for MIG1 (Heck *et al.*, 2016). Because SCL3 has a very similar paralogue in *M. truncatula* (Medtr4g076140, *SCL3-like1*), which is not mycorrhiza regulated and not modified by

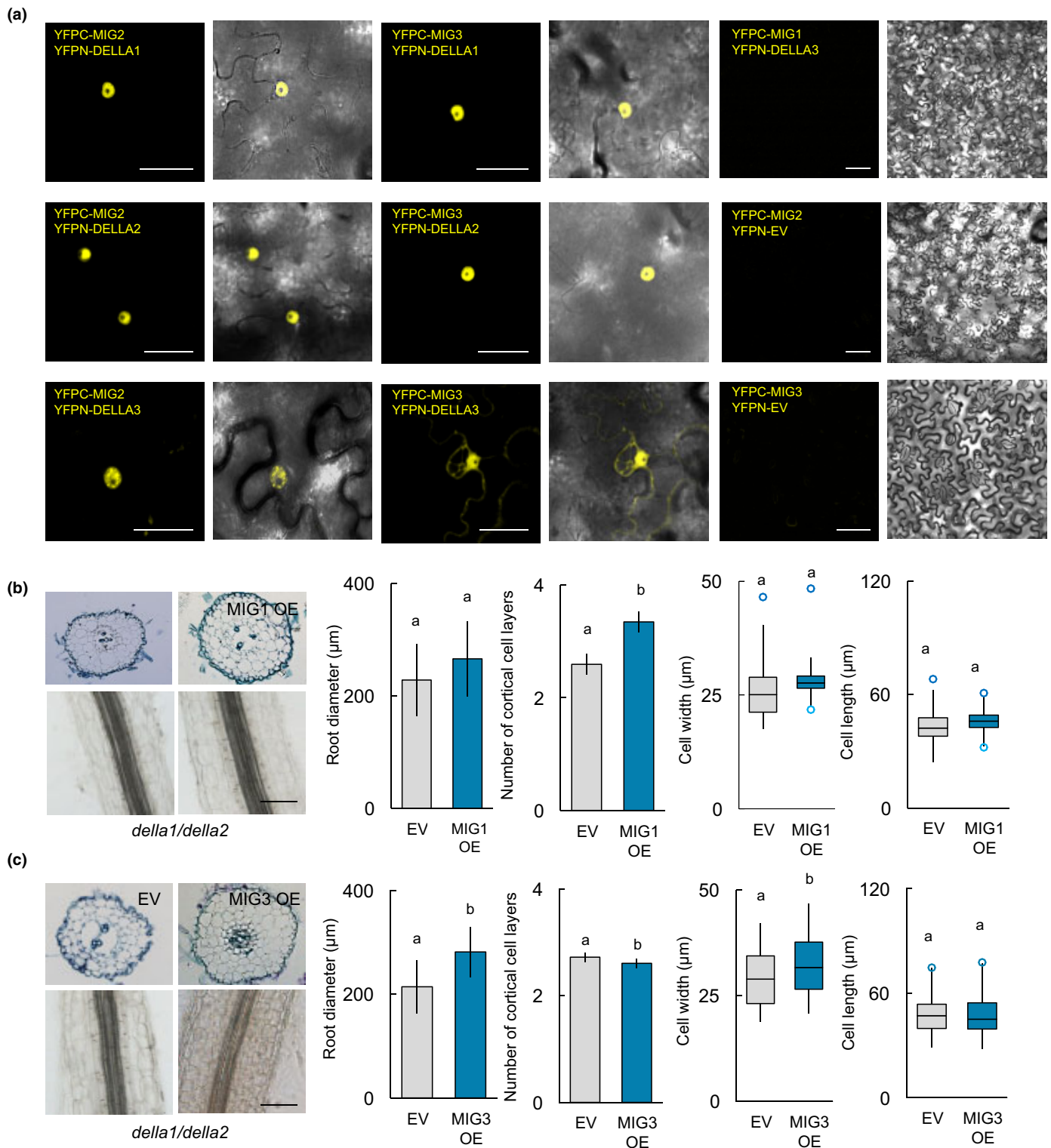


Fig. 4 MIG proteins require DELLA to control cortical cell width. (a) MIG2 and MIG3 interact with all DELLA proteins in the cell nucleus, as shown by bimolecular fluorescence complementation in *Nicotiana benthamiana* leaves. MIG1 does not interact with DELLA3. Bars, 50 μm . (b, c) Morphometric analyses (root diameter, number of cortical cell layers, and cortical cell width and length) of plants expressing either $2 \times P_{35S}::MIG1$ or $2 \times P_{35S}::MIG3$ in the *della1/della2* genetic background (ecotype R108) were carried out using the Fiji software package. Bars, 100 μm . (b) At least six biological replicates ($n = 6$) per treatment ($2 \times P_{35S}::MIG1$ or an empty vector (EV)), and n (roots) ≥ 60 and n (cells) ≥ 150 were analyzed. (c) Six biological replicates ($n = 6$) per treatment ($2 \times P_{35S}::MIG3$ or EV), and n (roots) ≥ 48 and n (cells) ≥ 120 were analyzed. Data represent mean (root diameter and number of cortical cell layers) \pm SD. Box-and-whisker plots (cell width and length) in this figure show the first, second and third quartiles, and the highest and lowest data points within a 1.5-interquartile range (IQR). Outliers are represented by blue circles. Significance was calculated according to the Mann–Whitney U -test. Different lower letters indicate significant difference ($P < 0.05$).

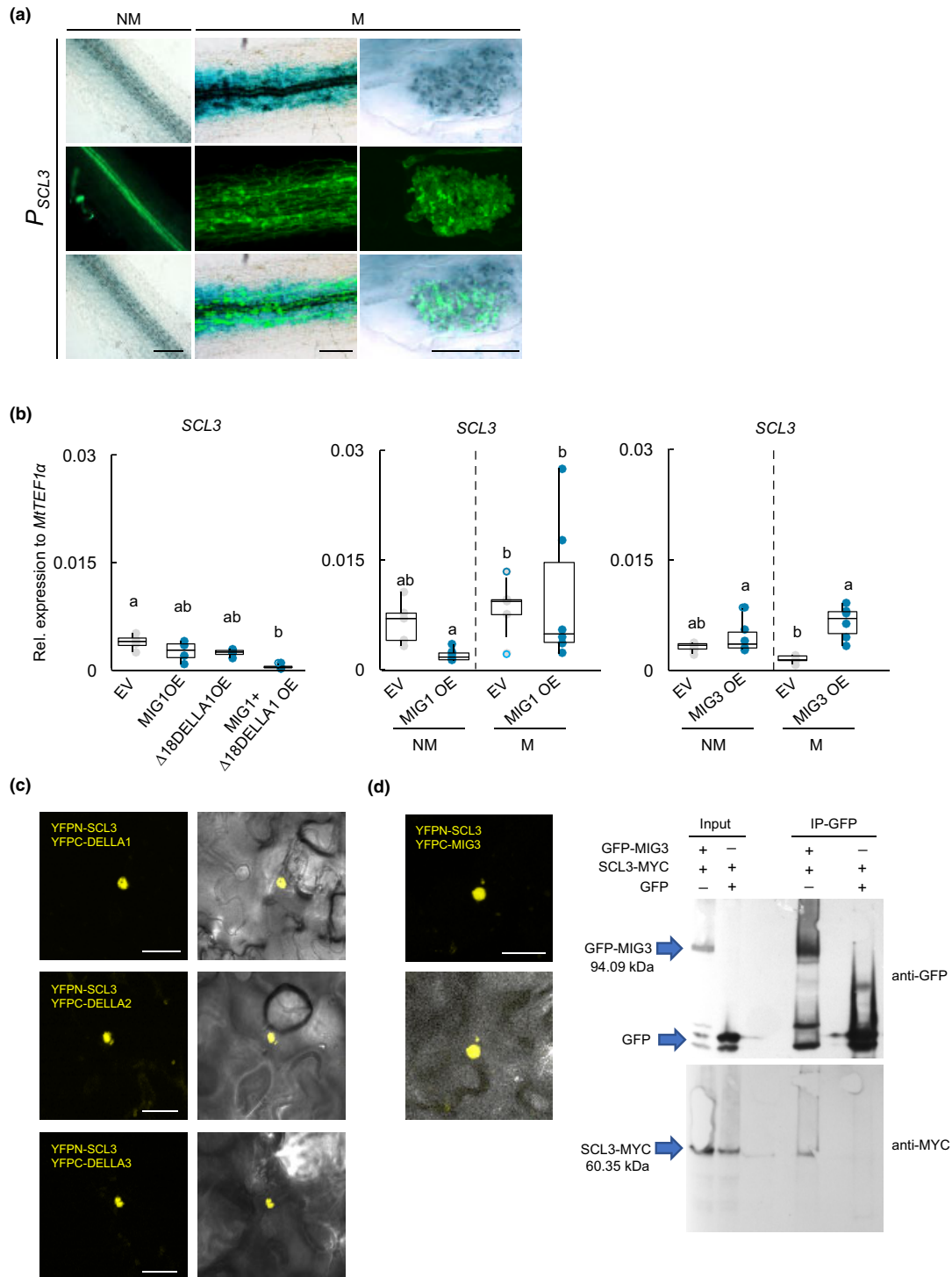
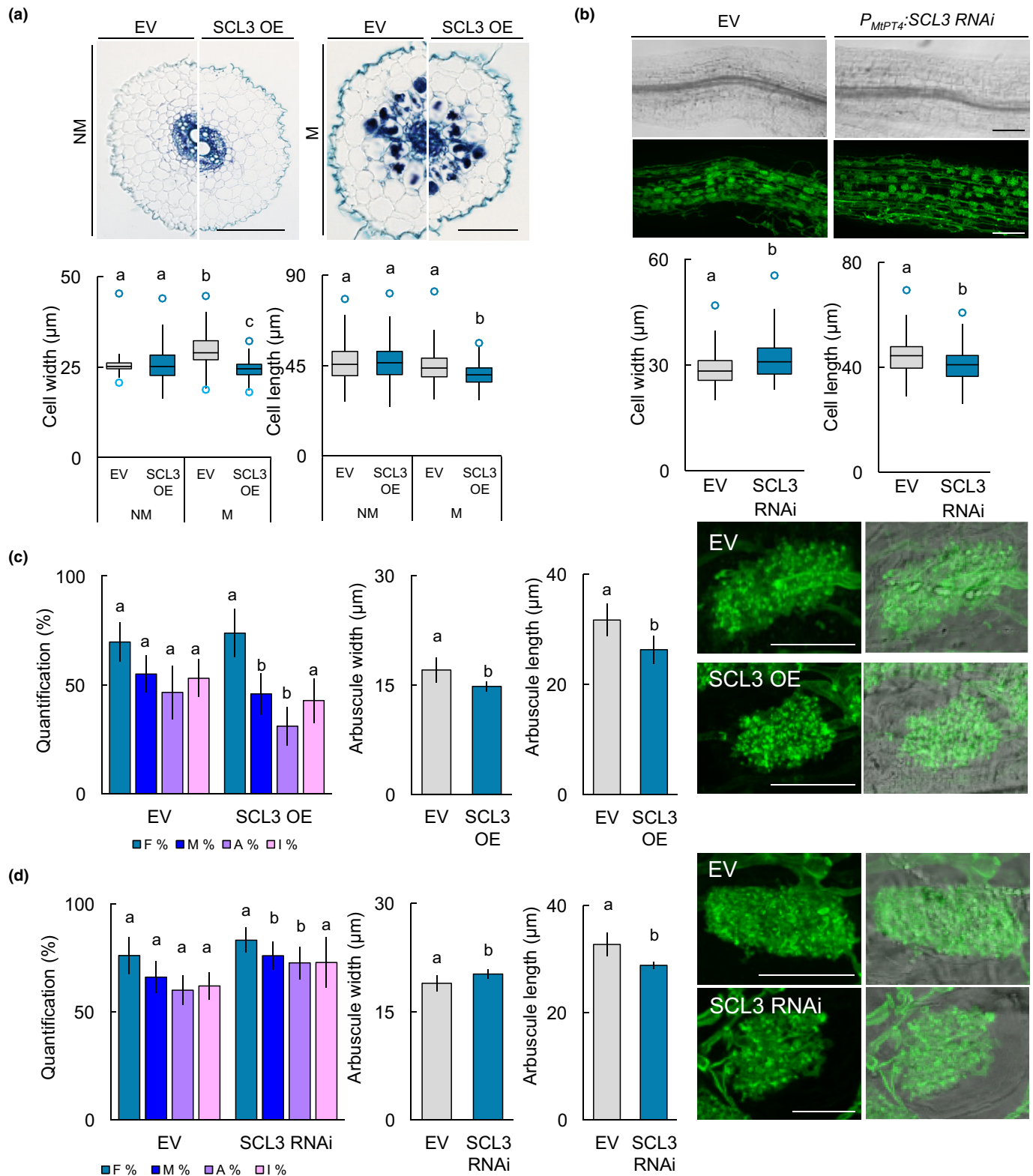


Fig. 5 *SCL3* is induced in arbuscule-containing cells and interacts with *MIG3*. (a) β -glucuronidase (*GUS*) promoter–reporter analysis for *SCL3*, using a 2-kb promoter fragment upstream from the ATG, is shown ($P_{MISCL3}::GUS$). Under nonmycorrhizal conditions the *SCL3* promoter is active in inner cortical cells. Under mycorrhizal conditions promoter activity is also observed in arbuscule-containing cells. The scale is 100 μ m and 25 μ m respectively. (b) Expression of *SCL3* in $2xP_{35S}::MIG1$, $2xP_{35S}::\Delta 18DELLA1$ and $2xP_{35S}::MIG1 + \Delta 18DELLA1$ overexpressing plants analyzed by quantitative real-time polymerase chain reaction (qRT-PCR) under nonmycorrhizal conditions ($n = 4$). *SCL3* transcript accumulation was also analyzed in roots ectopically expressing $2xP_{35S}::MIG1$ or $2xP_{35S}::MIG3$ with (M) and without (NM) mycorrhiza ($n = 6$). Box-and-whisker plots in this figure show the first, second and third quartiles, and the highest and lowest data points within a 1.5-interquartile range (IQR). Outliers are represented by blue circles. The Kolmogorov–Smirnov test was used to test for a normal distribution. Significance was calculated according to the Kruskal–Wallis test and the Tukey–Kramer *post-hoc* test. Different lowercase letters indicate significant differences ($P < 0.05$). (c) Interaction assays using bimolecular fluorescence complementation (BiFC) in *Nicotiana benthamiana* leaves between *SCL3* and all DELLA proteins was carried out. Bars, 50 μ m. (d) Interaction between *SCL3* and *MIG3* was shown by BiFC and co-immunoprecipitation (coIP) assays in *N. benthamiana* leaves. Bar, 50 μ m. For the coIP assay, *MIG3* was N-terminally tagged with eGFP and *SCL3* was C-terminally tagged with Myc. Free GFP was used as a control. Bars: (left panels) 100 μ m; (middle panels) 100 μ m; (right panels) 25 μ m.



ectopic expression of MIGs, we analyzed the specificity of *SCL3* silencing, showing that its expression was not affected (Fig. S9). Morphometric analyses of *SCL3*-silenced plants showed arbuscule-containing cells to be radially expanded and

longitudinally shorter (Fig. 6b). This is remarkable, because in *Arabidopsis* neither *scl3* nor *OESCL3* induced visible cortical cell changes in the wild-type genetic background but only in a constitutive dominant *DELLA* background (Heo *et al.*, 2011). There,

Fig. 6 Deregulation of *SCL3* shows it is a negative regulator of cell expansion in arbuscule-containing cells. (a) Radial root sections of nonmycorrhizal (NM) and mycorrhizal (M) roots expressing $2xP_{35S}::SCL3$ or an empty vector (EV) are shown. Bar, 100 μm . Morphometric analyses (cortical cell width and length) of roots were carried out using the Fiji software package. Six biological replicates per treatment were used, with n (roots) ≥ 15 per treatment and n (cells) ≥ 225 . Box-and-whisker plots (cell width and length) in this figure show the first, second and third quartiles, and the highest and lowest data points within a 1.5-interquartile range (IQR). Outliers are represented by blue circles. The Kolmogorov–Smirnov test was used to test for a normal distribution. Significance was calculated according to the Kruskal–Wallis test and the Tukey–Kramer *post-hoc* test. Different lowercase letters indicate significant difference ($P < 0.05$). (b) $P_{MtPT4}::SCL3$ RNAi silenced roots under the control of the *PT4* promoter were analyzed in longitudinal mycorrhizal root sections and compared to the corresponding EV. Bar, 100 μm . Morphometric analyses of the same roots (cortical cell width and length) were carried out using the Fiji software package. Six biological replicates ($n = 6$) per treatment ($P_{MtPT4}::SCL3$ RNAi or EV), n (roots) ≥ 20 and n (cells) ≥ 300 were measured. Box-and-whisker plots (cell width and length) in this figure show the first, second and third quartiles, and the highest and lowest data points within a 1.5-interquartile range (IQR). Outliers are represented by blue circles. Significance was calculated according to the Mann–Whitney *U*-Test. Different letters indicate significant difference ($P < 0.05$). (c, d) Quantification of mycorrhizal colonization was conducted according to the method described by Trouvelot *et al.* (1986). The parameters analyzed were frequency of colonization (F%), intensity of colonization (M%), abundance of arbuscules (A%) and abundance of intraradical hyphae (I%). Arbuscule length and width was measured using Fiji. For each treatment, the number of biological replicates were n (roots) = 6, and n (arbuscules) = 125 for both experiments ($2xP_{35S}::SCL3$ OE and $P_{MtPT4}::SCL3$ RNAi). Data represent mean \pm SD. Significance was calculated according to the two-tailed Student's *t*-test. Significance is given at $P < 0.05$ and is indicated by different lowercase letters. Representative arbuscules of each treatment stained with wheat germ agglutinin–fluorescein isothiocyanate conjugate (WGA-FITC) are shown. Bar, 25 μm .

scl3 reduced cell elongation and increased cell width, exacerbating the constitutive DELLA phenotype, while *OESCL3* restored the wild-type phenotype (Heo *et al.*, 2011). Thus, we can presume that in *M. truncatula* *SCL3* performs similar functions in arbuscule-containing cells, where DELLA activity is essential for arbuscule development and degeneration (Floss *et al.*, 2013, 2017; Pimprikar *et al.*, 2016).

We then investigated how the deregulation of *SCL3* impacted on mycorrhizal colonization and arbuscule development. In contrast to *MIG3*, overexpression of *SCL3* did not reduce the frequency or intensity of root colonization by *R. irregularis* (Figs 6c, S8). However, the number of arbuscules was reduced, as was their size, although expression of *MtPT4* was not altered. Consistently, silencing of *SCL3* increased arbuscule number and altered their shape, making them squarer, concomitant with an increase in *MtPT4* expression (Figs 6d, S8). Altogether, these results suggest that *MIG3* and *SCL3* contribute to restraining cortical cell expansion of colonized cells and consequently negatively impact on the size of arbuscules. However, *MIG3*, in addition, plays a role in cell expansion under nonsymbiotic conditions independent of *SCL3*, thus suggesting the involvement of other as-yet unidentified downstream transcription factors.

Discussion

Observing the arbuscules of *Glomites rhyaniensis* in the cortical cells of fossilised *Aglaophyton major* plants from the Devonian period (*c.* 400 Myr old; Berbee *et al.*, 2017) it becomes obvious how little the morphology of these structures has changed in their evolution to modern arbuscules. This clearly emphasizes the importance of this interface for the functioning of a symbiosis that engages > 80% of all land plants (Smith & Read, 2008). But if, in addition, we consider the fact that arbuscules are ephemeral structures that are built and deconstructed within days (Scannerini & Bonfante-Fasolo, 1983; Toth & Miller, 1984; Pumplun *et al.*, 2012), then it is easy to imagine that extremely conserved and complex molecular mechanisms lie behind this developmental process.

However, it went unnoticed for a relatively long time that transcription factors known to control morphological processes

of root cortical cells could be involved in arbuscule development. This is partly due to the fact that colonization of the cortex by AM fungi does not provoke the dramatic tissue neoplasia observed in other root–microbial associations, such as Rhizobia-induced nodules or nematode-induced knots. Another contributing factor is that most of the studies and mutant phenotypes for those transcription factors had been identified in Arabidopsis, which is one of the few plants that is unable to engage in arbuscular mycorrhizal symbiosis. Furthermore, recent studies have shown that root developmental processes such as lateral root formation and root apical meristem activity, which are critical for endosymbiosis and are positively regulated by GA in Arabidopsis, are oppositely controlled in *M. truncatula* (Fonouni-Farde *et al.*, 2019). The discovery and characterization of RAM1 (Wang *et al.*, 2012; Park *et al.*, 2015; Pimprikar *et al.*, 2016) and subsequent identification of many other GRAS transcription factors as central regulators of arbuscule development in plants forming arbuscular mycorrhiza started to change this picture (Floss *et al.*, 2013; Yu *et al.*, 2014; Xue *et al.*, 2015; Heck *et al.*, 2016; Hartmann *et al.*, 2019; Ho-Plagaro *et al.*, 2019). And interestingly, several of these transcription factors specific for mycorrhiza development were shown to be absent in Arabidopsis, emphasizing the need to extend the studies of root development to other plants.

Here we further contribute to the knowledge of how GRAS transcription factors impact arbuscule development, through the characterization of three new GRAS transcription factors, *MIG2*, *MIG3* and *SCL3*, in *M. truncatula*. All of these genes are induced in arbuscule-containing cells, and their functional characterization has shown that, like *MIG1*, they are regulators of cortical cell size. However, while *MIG2* and *MIG1* are positive regulators, *MIG3* and *SCL3* negatively impact cortical cell size. Because *MIG1* and *MIG2* have almost identical phenotypes, the fact that *MIG1* evolved to be a positive regulator that is specifically expressed in arbuscule-containing cells is intriguing. We hypothesize that the answer lies in the promoter of the genes, because *MIG1* (and *MIG3*) contains, in contrast to *MIG2*, the P1BS regulatory motif (Rubio *et al.*, 2001). This element, together with the CTTC motif, could allow the coordination of *MIG1*

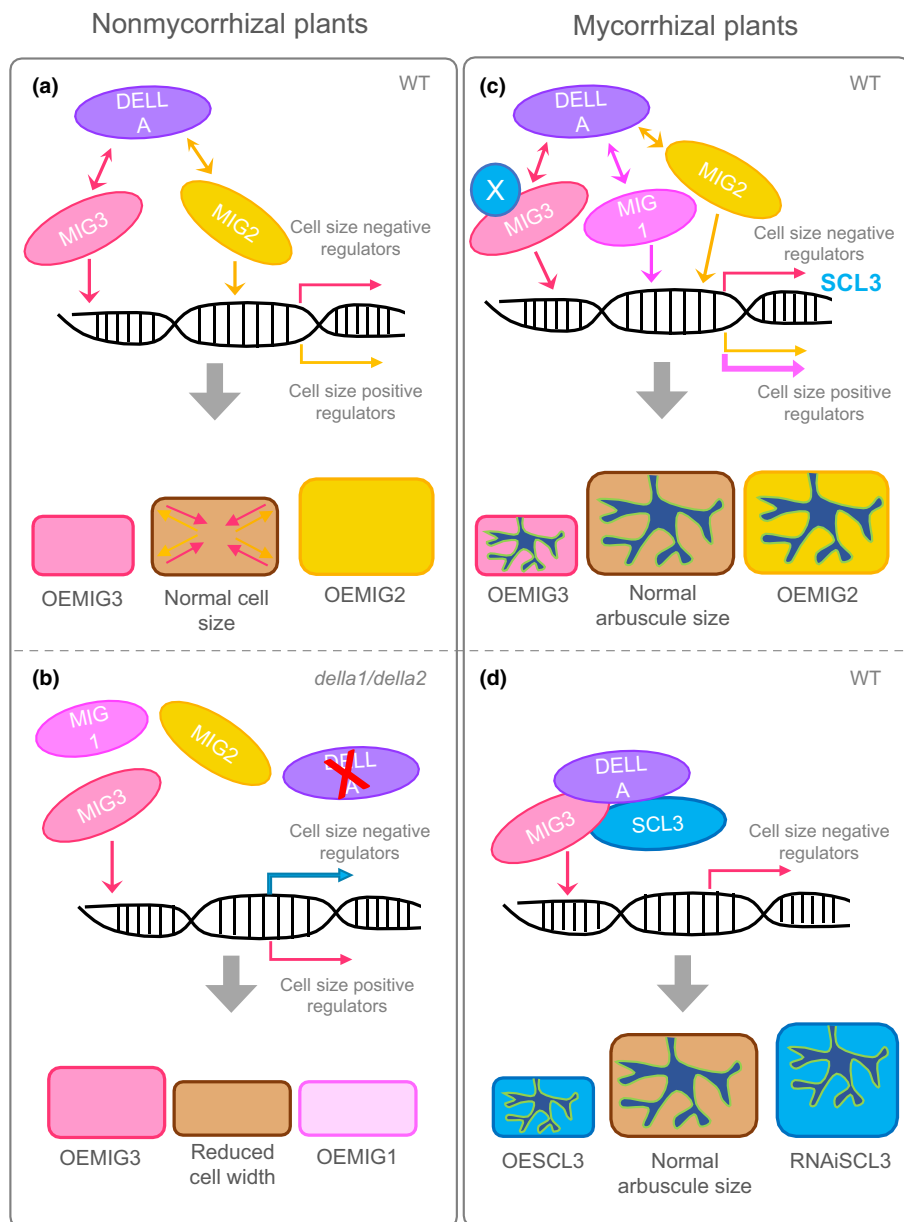


Fig. 7 Hypothetical model of cortical cell size regulation in *Medicago truncatula* by the interplay of MIGs, DELLA and SCL3 GRAS transcription factors. (a) In wild-type nonmycorrhizal plants, cortical cell size is regulated by positive and negative regulators. The GRAS transcription factor MIG3 induces the expression of negative regulators in a DELLA-dependent manner, consequently restraining cell expansion. Under those circumstances, MIG2 acts on cell size positive regulators, and its overexpression increases cell size. (b) In a *della1/della2* genetic background, cortical cells are thinner, likely because transcription factors acting on radial cell expansion (such as MIG2) are no longer active. In support of that hypothesis, overexpression of MIG1 is no longer a positive regulator of cell expansion. Surprisingly, in that genetic background, overexpression of MIG3 causes cell expansion. Thus, we hypothesize that MIG3 also acts in a DELLA-independent manner on positive regulators of cell expansion. (c) During mycorrhizal colonization cortical cells harboring arbuscules expand through the expression of MIG1 (and MIG2) in a DELLA-dependent manner. Cell expansion is constrained by the action of MIG3, which activates, likely in combination with an unknown transcription factor X, a second negative regulator, SCL3. SCL3 could itself be the transcription factor X. Overexpression of MIG3 therefore reduces cell size and consequently arbuscule size. (d) SCL3 together with MIG3 and DELLA counteract the positive effect of MIG1 on cell expansion, resulting in smaller cells and thus smaller arbuscules. Silencing SCL3 in arbuscule-containing cells is no longer able to counteract this effect, and cells are radially expanded and shorter.

expression with the phosphate starvation response in arbuscule-containing cells, linking cell morphology to the main function of arbuscules – the phosphate exchange.

We have shown previously that GA is able to counteract all enhancing effects of MIG1 on cortical cell development and that a constitutive active DELLA was able to restore the wild-type arbuscule phenotype lost in *MIG1* silenced plants. Furthermore, constitutive active DELLA showed more severe but identical phenotypes to *MIG1* overexpressing plants regarding cortical radial cell expansion and cell layers, suggesting that DELLA and MIG1 had overlapping functions in those developmental changes (Heck *et al.*, 2016). However, here we show that DELLA is only required for changes regarding radial cell expansion, but not for the increase in cortical cell divisions mediated by MIG1. Surprisingly, given the high degree of conservation among MIG proteins, MIG3 turned out to be a negative regulator of cell

expansion, especially under mycorrhizal conditions, thus counteracting MIG1 and MIG2. This somewhat indicates that MIG3 could act by promoting gibberellin signaling and opposing DELLA function. The interactions of MIG1 and MIG3 with DELLA and the fact that in the *della1della2* genetic background, MIG1 no longer promotes cell expansion while MIG3 is in that context a positive regulator, supports a model of two transcriptional complexes acting on the promoter of cell expansion executor genes.

In order to start identifying such executors, we focussed on SCL3, which has been shown in *Arabidopsis* (*AtSCL3*) to be a positive regulator of GA signaling (Heo *et al.*, 2011; Zhang *et al.*, 2011) despite being repressed by GA and induced by DELLA (Zentella *et al.*, 2007). *AtSCL3* positively affects GA signaling by antagonizing DELLA, acting as its attenuator in the endodermis to control cell elongation (Heo *et al.*, 2011; Zhang *et al.*, 2011).

In Arabidopsis, SCR together with SHR positively control *AtSCL3* expression in the endodermis (Di Laurenzio *et al.*, 1996; Pysh *et al.*, 1999). However, the promoter of *SCR* has a broader expression distribution in *M. truncatula* than in Arabidopsis, localizing not only in the endodermis but also in the cells of the inner cortex (Dong *et al.*, 2021). Accordingly, *M. truncatula SCL3* also shows expression in cells of the inner cortex, in contrast to observations in Arabidopsis, where *AtSCL3* is basically only expressed in the endodermis (Pysh *et al.*, 1999). These differences are not surprising as *M. truncatula* contains several more layers of cortical cells than Arabidopsis, and SHR/SCR are known to be responsible for generating additional periclinal divisions in combination with GA signaling during middle cortex formation (Helariutta *et al.*, 2000; Paquette & Benfey, 2005). Furthermore, other species showing multi cortical layers, such as rice, have been shown to also have a less restricted pattern of *SHR* gene movement (Wu *et al.*, 2014; Henry *et al.*, 2017). Analogous to findings in Arabidopsis, where *AtSCL3* constraining effects on radial cell expansion are only visible in a constitutive active DELLA background (Heo *et al.*, 2011), in *M. truncatula*, *SCL3* overexpression only negatively impacted radial cell expansion under mycorrhizal conditions, where DELLA and MIG1 promote cell expansion of arbuscule-containing cells. Congruently, in our experiments *SCL3* RNAi increased cell width and reduced cell elongation coincident with the phenotype of *scl3* in Arabidopsis in a dominant DELLA background (Heo *et al.*, 2011) and similar to the phenotype of a constitutive active DELLA in *M. truncatula* (Heck *et al.*, 2016).

As in Arabidopsis, *SCL3* in *M. truncatula* interacts with DELLA. Because neither DELLA nor *AtSCL3* contain any known DNA binding domains, it was proposed that they would act in a complex with other transcription factors containing DNA binding domains (Zhang *et al.*, 2011). All MIG proteins have long amino termini with putative DNA binding domains that could mediate the direct binding to downstream targets (Heck *et al.*, 2016). Interestingly, *SCL3* interacts not only with DELLA but also with MIG3 in the nucleus (but not with MIG1 or MIG2), suggesting they could be part of a transcriptional complex. Ectopic expression of MIG1 or MIG2 in mycorrhizal plants did not further promote increases in cell size nor in arbuscule size, likely because under those conditions the maximum cell size is achieved. By contrast, MIG3 and *SCL3* negatively affected both.

A possible scenario for the control of cortical cell size in *M. truncatula* is depicted in Fig. 7. Under nonmycorrhizal conditions, MIG3 acts as a negative regulator of cell expansion in a DELLA-dependent manner by inducing the expression of negative regulators of cell expansion and counteracting the positive regulation by MIG2. However, MIG3 also has a DELLA-independent role on cell expansion, inducing unknown positive regulators, as demonstrated by its overexpression in a *della1/della2* background, although it should be kept in mind that a third DELLA3, of unknown function, is present in that genetic background. MIG1, in a DELLA-dependent manner, could be acting on the promoter of those same genes as a repressor, as shown by its negative regulation of *SCL3* in the presence of a constitutive

DELLA. However, it is also likely that MIG1, as well as MIG2, are activators of positive regulators of cell expansion. During mycorrhizal colonization, cortical cells harbouring arbuscules expand through the expression of MIG1 (and MIG2) in a DELLA-dependent manner. Cell expansion is constrained by the action of MIG3, which activates, likely in combination with an unknown transcription factor X that is only present in mycorrhizal conditions, a second negative regulator, *SCL3*. The possibility that *SCL3* is the transcription factor X itself cannot be excluded. Under the experimental conditions described in this study, it is difficult to obtain a better time-and-space resolution of the expression/action of all transcriptional regulators here analyzed, given the fact that arbuscules are dynamic and are constantly formed and disassembled, and that different regions of the same root might have arbuscules in different developmental stages. However, we feel that our results will help to further untangle the complex regulatory circuits coordinating arbuscule formation and root cell morphology.

In summary, we have shown here that regulation of cell size in root cortical cells that harbour arbuscules is controlled by a network of GRAS transcription factors, and we hypothesize that they act in a coordinated manner to adjust plant development to the dynamic advance of the symbiosis. We describe two negative regulators of cell expansion, MIG3 and *SCL3*, that act in concert with the central regulator DELLA to restrain radial cell expansion. As in a tug of war, when MIG1 is induced in arbusculated cells, it promotes, together with DELLA, cortical radial cell expansion to accommodate the developing arbuscule, and antagonizes the function of MIG3 and *SCL3*. It is likely that MIG1 and MIG3 compete for binding to DELLA and likely for binding to the promoter of the same target genes, one of which might be *SCL3* itself. This study advances the knowledge of plant regulators of root development in legume plants and, additionally, knowledge of their involvement in regulating one of the most widespread and important plant symbioses on earth. Further studies are now required to understand the dynamic of these interaction complexes in cells containing arbuscules to unravel the mechanisms that balance the formation of different transcriptional complexes and ultimately decide the size and shape of cortical cells.


Acknowledgements

We would like to acknowledge our colleagues Dr M. Bastmeyer and Dr R. Fischer for their helpful discussions. We thank Dr M. Harrison for providing seeds of the double DELLA mutant, Dr G. Jürges for advice regarding the preparation of the cross sections, and S. Heupel for technical support. This work was supported by KIT funding. The authors declare no competing interests. Open access funding enabled and organized by ProjektDEAL.

Author contributions

NR and CS designed the experiments and wrote the manuscript. CS, CH, SV, JS, EE and DS carried out the experiments.

ORCID

Natalia Requena  <https://orcid.org/0000-0001-5406-0015>

Data availability

All data are available in the manuscript or will be made available upon request.

References

- Balestrini R, Cosgrove DJ, Bonfante P. 2005. Differential location of alpha-expansin proteins during the accommodation of root cells to an arbuscular mycorrhizal fungus. *Planta* 220: 889–899.
- Benedito VA, Torres-Jerez I, Murray JD, Andriankaja A, Allen S, Kakar K, Wandrey M, Verdier J, Zuber H, Ott T *et al.* 2008. A gene expression atlas of the model legume *Medicago truncatula*. *The Plant Journal* 55: 504–513.
- Berbee ML, James TY, Strullu-Derrien C. 2017. Early diverging fungi: diversity and impact at the dawn of terrestrial life. *Annual Review of Microbiology* 71: 41–60.
- Berta G, Trotta A, Fusconi A, Hooker JE, Munro M, Atkinson D, Giovannetti M, Morini S, Fortuna P, Tisserant B *et al.* 1995. Arbuscular mycorrhizal induced changes to plant growth and root system morphology in *Prunus cerasifera*. *Tree Physiology* 15: 281–293.
- Boisson-Dernier A, Chabaud M, Garcia F, Becard G, Rosenberg C, Barker DG. 2001. *Agrobacterium rhizogenes*-transformed roots of *Medicago truncatula* for the study of nitrogen-fixing and endomycorrhizal symbiotic associations. *Molecular Plant-Microbe Interactions* 14: 695–700.
- Bravo A, York T, Pumphlin N, Mueller LA, Harrison MJ. 2016. Genes conserved for arbuscular mycorrhizal symbiosis identified through phylogenomics. *Nature Plants* 2: 15208.
- Chen A, Gu M, Sun S, Zhu L, Hong S, Xu G. 2011. Identification of two conserved cis-acting elements, MYCS and P1BS, involved in the regulation of mycorrhiza-activated phosphate transporters in eudicot species. *New Phytologist* 189: 1157–1169.
- Choi J, Lee T, Cho J, Servante EK, Pucker B, Summers W, Bowden S, Rahimi M, An K, An G *et al.* 2020. The negative regulator SMAX1 controls mycorrhizal symbiosis and strigolactone biosynthesis in rice. *Nature Communications* 11: 2114.
- Choi JW, Lim J. 2016. Control of asymmetric cell divisions during root ground tissue maturation. *Molecules and Cells* 39: 524–529.
- Devers EA, Teply J, Reinert A, Gaude N, Krajinski F. 2013. An endogenous artificial microRNA system for unraveling the function of root endosymbioses related genes in *Medicago truncatula*. *BMC Plant Biology* 13: 82.
- Di Lorenzo L, Wysocka-Diller J, Malamy JE, Pysh L, Helariutta Y, Freshour G, Hahn MG, Feldmann KA, Benfey PN. 1996. The SCARECROW gene regulates an asymmetric cell division that is essential for generating the radial organization of the *Arabidopsis* root. *Cell* 86: 423–433.
- Dong W, Zhu Y, Chang H, Wang C, Yang J, Shi J, Gao J, Yang W, Lan L, Wang Y *et al.* 2021. An SHR-SCR module specifies legume cortical cell fate to enable nodulation. *Nature* 589: 586–590.
- El Ghachtouli N, Martin-Tanguy J, Paynot M, Gianinazzi S. 1996. First report of the inhibition of arbuscular mycorrhizal infection of *Pisum sativum* by specific and irreversible inhibition of polyamine biosynthesis or by gibberellic acid treatment. *FEBS Letters* 385: 189–192.
- Floss DS, Gomez SK, Park HJ, MacLean AM, Muller LM, Bhattarai KK, Levesque-Tremblay V, Maldonado-Mendoza IE, Harrison MJ. 2017. A transcriptional program for arbuscule degeneration during AM symbiosis is regulated by MYB1. *Current Biology* 27: 1206–1212.
- Floss DS, Levesque-Tremblay V, Park HJ, Harrison MJ. 2016. DELLA proteins regulate expression of a subset of AM symbiosis-induced genes in *Medicago truncatula*. *Plant Signal & Behavior* 11: e1162369.
- Floss DS, Levy JG, Levesque-Tremblay V, Pumphlin N, Harrison MJ. 2013. DELLA proteins regulate arbuscule formation in arbuscular mycorrhizal symbiosis. *Proceedings of the National Academy of Sciences, USA* 110: E5025–E5034.
- Fonouni-Farde C, Miassod A, Laffont C, Morin H, Bendahmane A, Diet A, Frugier F. 2019. Gibberellins negatively regulate the development of *Medicago truncatula* root system. *Scientific Reports* 9: 2335.
- Foo E, Ross JJ, Jones WT, Reid JB. 2013. Plant hormones in arbuscular mycorrhizal symbioses: an emerging role for gibberellins. *Annals of Botany* 111: 769–779.
- Gaude N, Bortfeld S, Duensing N, Lohse M, Krajinski F. 2012. Arbuscule-containing and non-colonized cortical cells of mycorrhizal roots undergo extensive and specific reprogramming during arbuscular mycorrhizal development. *The Plant Journal* 69: 510–528.
- Gobbato E, Marsh J, Vernié T, Wang E, Maillet F, Kim J, Miller J, Sun J, Bano S, Ratet P *et al.* 2012. A GRAS-type transcription factor with a specific function in mycorrhizal signaling. *Current Biology* 22: 2236–2241.
- Gomez SK, Javot H, Deewatthanawong P, Torres-Jerez I, Tang Y, Blancaflor EB, Udvardi MK, Harrison MJ. 2009. *Medicago truncatula* and *Glomus intraradices* gene expression in cortical cells harboring arbuscules in the arbuscular mycorrhizal symbiosis. *BMC Plant Biology* 9: 10.
- Guether M, Balestrini R, Hannah M, He J, Udvardi MK, Bonfante P. 2009. Genome-wide reprogramming of regulatory networks, transport, cell wall and membrane biogenesis during arbuscular mycorrhizal symbiosis in *Lotus japonicus*. *New Phytologist* 182: 200–212.
- Hartmann RM, Schaepe S, Nubel D, Petersen AC, Bertolini M, Vasilev J, Kuster H, Hohnjec N. 2019. Insights into the complex role of GRAS transcription factors in the arbuscular mycorrhiza symbiosis. *Scientific Reports* 9: 3360.
- Heck C, Kuhn H, Heidt S, Walter S, Rieger N, Requena N. 2016. Symbiotic fungi control plant root cortex development through the novel GRAS transcription factor MIG1. *Current Biology* 26: 2770–2778.
- Helariutta Y, Fukaki H, Wysocka-Diller J, Nakajima K, Jung J, Sena G, Hauser MT, Benfey PN. 2000. The SHORT-ROOT gene controls radial patterning of the *Arabidopsis* root through radial signaling. *Cell* 101: 555–567.
- Henry S, Dievart A, Divol F, Pauluzzi G, Meynard D, Swarup R, Wu S, Gallagher KL, Perin C. 2017. SHR overexpression induces the formation of supernumerary cell layers with cortex cell identity in rice. *Developmental Biology* 425: 1–7.
- Heo JO, Chang KS, Kim IA, Lee MH, Lee SA, Song SK, Lee MM, Lim J. 2011. Funneling of gibberellin signaling by the GRAS transcription regulator scarecrow-like 3 in the *Arabidopsis* root. *Proceedings of the National Academy of Sciences, USA* 108: 2166–2171.
- Hogekamp C, Arndt D, Pereira PA, Becker JD, Hohnjec N, Kuster H. 2011. Laser microdissection unravels cell-type-specific transcription in arbuscular mycorrhizal roots, including CAAT-box transcription factor gene expression correlating with fungal contact and spread. *Plant Physiology* 157: 2023–2043.
- Hohnjec N, Vieweg MF, Puhler A, Becker A, Kuster H. 2005. Overlaps in the transcriptional profiles of *Medicago truncatula* roots inoculated with two different *Glomus* fungi provide insights into the genetic program activated during arbuscular mycorrhiza. *Plant Physiology* 137: 1283–1301.
- Ho-Plagaro T, Molinero-Rosales N, Farina Flores D, Villena Diaz M, Garcia-Garrido JM. 2019. Identification and expression analysis of GRAS transcription factor genes involved in the control of arbuscular mycorrhizal development in tomato. *Frontiers in Plant Science* 10: 268.
- Jiang C, Gao X, Liao L, Harberd NP, Fu X. 2007. Phosphate starvation root architecture and anthocyanin accumulation responses are modulated by the gibberellin-DELLA signaling pathway in *Arabidopsis*. *Plant Physiology* 145: 1460–1470.
- Jiang Y, Xie Q, Wang W, Yang J, Zhang X, Yu N, Zhou Y, Wang E. 2018. *Medicago* AP2-domain transcription factor WR15a is a master regulator of lipid biosynthesis and transfer during mycorrhizal symbiosis. *Molecular Plant* 11: 1344–1359.
- Krajinski F, Courty PE, Sieh D, Franken P, Zhang H, Bucher M, Gerlach N, Kryvoruchko I, Zoeller D, Udvardi M *et al.* 2014. The H⁺-ATPase HA1 of *Medicago truncatula* is essential for phosphate transport and plant growth during arbuscular mycorrhizal symbiosis. *Plant Cell* 26: 1808–1817.
- Kuhn H, Kuster H, Requena N. 2010. Membrane steroid-binding protein 1 induced by a diffusible fungal signal is critical for mycorrhization in *Medicago truncatula*. *New Phytologist* 185: 716–733.

- Kumar S, Stecher G, Tamura K. 2016. MEGA7: molecular evolutionary genetics analysis v.7.0 for bigger datasets. *Molecular Biology and Evolution* 33: 1870–1874.
- Lanfranco L, Fiorilli V, Gutjahr C. 2018. Partner communication and role of nutrients in the arbuscular mycorrhizal symbiosis. *New Phytologist* 220: 1031–1046.
- Lota F, Wegmuller S, Buer B, Sato S, Brautigam A, Hanf B, Bucher M. 2013. The cis-acting CTTC-P1BS module is indicative for gene function of LjVT112, a Qb-SNARE protein gene that is required for arbuscule formation in *Lotus japonicus*. *The Plant Journal* 74: 280–293.
- Luginbuehl LH, Menard GN, Kurup S, Van Erp H, Radhakrishnan GV, Brekspear A, Oldroyd GED, Eastmond PJ. 2017. Fatty acids in arbuscular mycorrhizal fungi are synthesized by the host plant. *Science* 356: 1175–1178.
- Luginbuehl LH, Oldroyd GED. 2017. Understanding the Arbuscule at the heart of endomycorrhizal symbioses in plants. *Current Biology* 27: R952–R963.
- Nakagawa T, Suzuki T, Murata S, Nakamura S, Hino T, Miao K, Tabata R, Kawai T, Tanaka K, Niwa Y *et al.* 2007. Improved Gateway binary vectors: high-performance vectors for creation of fusion constructs in transgenic analysis of plants. *Bioscience, Biotechnology, and Biochemistry* 71: 2095–2100.
- Paquette AJ, Benfey PN. 2005. Maturation of the ground tissue of the root is regulated by gibberellin and SCARECROW and requires SHORT-ROOT. *Plant Physiology* 138: 636–640.
- Park HJ, Floss DS, Levesque-Tremblay V, Bravo A, Harrison MJ. 2015. Hyphal branching during arbuscule development requires reduced arbuscular mycorrhizal. *Plant Physiology* 169: 2774–2788.
- Pimprikar P, Carbonnel S, Paries M, Katzer K, Klingl V, Bohmer M, Karl L, Floss D, Harrison M, Parniske M *et al.* 2016. A CCaMK-CYCLOPS-DELLA complex activates transcription of RAM1 to regulate arbuscule branching. *Current Biology* 26: 987–998.
- Pumplin N, Zhang X, Noar RD, Harrison MJ. 2012. Polar localization of a symbiosis-specific phosphate transporter is mediated by a transient reorientation of secretion. *Proceedings of the National Academy of Sciences, USA* 109: E665–672.
- Pysh LD, Wysocka-Diller JW, Camilleri C, Bouchez D, Benfey PN. 1999. The GRAS gene family in *Arabidopsis*: sequence characterization and basic expression analysis of the SCARECROW-LIKE genes. *The Plant Journal* 18: 111–119.
- Quandt HJ, Pühler A, Broer I. 1993. Transgenic root nodules of *Vicia hirsuta*: a fast and efficient system for the study of gene expression in indeterminate-type nodules. *Molecular Plant-Microbe Interactions* 6: 699–706.
- Rech SS, Heidt S, Requena N. 2013. A tandem Kunitz protease inhibitor (KPI106)-serine carboxypeptidase (SCP1) controls mycorrhiza establishment and arbuscule development in *Medicago truncatula*. *The Plant Journal* 75: 711–725.
- Redecker D, Morton JB, Bruns TD. 2000. Ancestral lineages of arbuscular mycorrhizal fungi (Glomales). *Molecular Phylogenetics and Evolution* 14: 276–284.
- Remy W, Taylor TN, Hass H, Kerp H. 1994. Four hundred-million-year-old vesicular arbuscular mycorrhizae. *Proceedings of the National Academy of Sciences, USA* 91: 11841–11843.
- Rubio V, Linhares F, Solano R, Martin AC, Iglesias J, Leyva A, Paz-Ares J. 2001. A conserved MYB transcription factor involved in phosphate starvation signaling both in vascular plants and in unicellular algae. *Genes & Development* 15: 2122–2133.
- Russo G, Carotenuto G, Fiorilli V, Volpe V, Chiappello M, Van Damme D, Genre A. 2019a. Ectopic activation of cortical cell division during the accommodation of arbuscular mycorrhizal fungi. *New Phytologist* 221: 1036–1048.
- Russo G, Carotenuto G, Fiorilli V, Volpe V, Faccio A, Bonfante P, Chabaud M, Chiappello M, Van Damme D, Genre A. 2019b. TPLATE recruitment reveals endocytic dynamics at sites of symbiotic interface assembly in arbuscular mycorrhizal interactions. *Frontiers in Plant Science* 10: 1628.
- Scannerini S, Bonfante-Fasolo P. 1983. Comparative ultrastructural analysis of mycorrhizal associations. *Canadian Journal of Botany* 61: 917–943.
- Schenck N, Smith G. 1982. Additional new and unreported species of mycorrhizal fungi (Endogonaceae) from Florida. *Mycologia* 74: 77–92.
- Simon L, Levesque RC, Lalonde M. 1993. Identification of endomycorrhizal fungi colonizing roots by fluorescent single-strand conformation polymorphism-polymerase chain reaction. *Applied and Environment Microbiology* 59: 4211–4215.
- Smith SE, Read DJ. 2008. *Mycorrhizal symbiosis*. San Diego, CA, USA: Academic Press.
- Smith SE, Smith FA. 2011. Roles of arbuscular mycorrhizas in plant nutrition and growth: new paradigms from cellular to ecosystem scales. *Annual Review of Plant Biology* 62: 227–250.
- Spatafora JW, Chang Y, Benny GL, Lazarus K, Smith ME, Berbee ML, Bonito G, Corradi N, Grigoriev I, Gryganskyi A *et al.* 2016. A phylum-level phylogenetic classification of zygomycete fungi based on genome-scale data. *Mycologia* 108: 1028–1046.
- Toth R, Miller RM. 1984. Dynamics of arbuscule development and degeneration in a *Zea mays* mycorrhiza. *American Journal of Botany* 71: 449–460.
- Trouvelot A, Kough J, Gianinazzi-Pearson V. 1986. *Estimation of VA mycorrhizal infection levels. Research for methods having a functional significance. Physiological and genetical aspects of mycorrhizae*. Versailles, France: Service des Publications INRA, 223–232.
- Voinnet O, Rivas S, Mestre P, Baulcombe D. 2003. An enhanced transient expression system in plants based on suppression of gene silencing by the p19 protein of tomato bushy stunt virus. *The Plant Journal* 33: 949–956.
- Volpe V, Dell'Aglio E, Giovannetti M, Ruberti C, Costa A, Genre A, Guether M, Bonfante P. 2013. An AM-induced, MYB-family gene of *Lotus japonicus* (LjMAMI) affects root growth in an AM-independent manner. *The Plant Journal* 73: 442–455.
- Walter M, Chaban C, Schütze K, Batistic O, Weckermann K, Näke C, Blazevic D, Grefen C, Schumacher K, Oecking C *et al.* 2004. Visualization of protein interactions in living plant cells using bimolecular fluorescence complementation. *The Plant Journal* 40: 428–438.
- Wang E, Schornack S, Marsh JF, Gobbato E, Schwessinger B, Eastmond P, Schultze M, Kamoun S, Oldroyd GE. 2012. A common signaling process that promotes mycorrhizal and oomycete colonization of plants. *Current Biology* 22: 2242–2246.
- Wu S, Lee CM, Hayashi T, Price S, Divol F, Henry S, Pauluzzi G, Perin C, Gallagher KL. 2014. A plausible mechanism, based upon short-root movement, for regulating the number of cortex cell layers in roots. *Proceedings of the National Academy of Sciences, USA* 111: 16184–16189.
- Wulf A, Manthey K, Doll J, Perlick AM, Linke B, Bekel T, Meyer F, Franken P, Kuster H, Krajinski F. 2003. Transcriptional changes in response to arbuscular mycorrhiza development in the model plant *Medicago truncatula*. *Molecular Plant-Microbe Interactions* 16: 306–314.
- Xue L, Cui H, Buer B, Vijayakumar V, Delaux PM, Junkermann S, Bucher M. 2015. Network of GRAS transcription factors involved in the control of arbuscule development in *Lotus japonicus*. *Plant Physiology* 167: 854–871.
- Xue L, Klinnawee L, Zhou Y, Saridis G, Vijayakumar V, Brands M, Dormann P, Gigolashvili T, Turck F, Bucher M. 2018. AP2 transcription factor CBX1 with a specific function in symbiotic exchange of nutrients in mycorrhizal *Lotus japonicus*. *Proceedings of the National Academy of Sciences, USA* 115: E9239–E9246.
- Yu N, Luo D, Zhang X, Liu J, Wang W, Jin Y, Dong W, Liu J, Liu H, Yang W *et al.* 2014. A DELLA protein complex controls the arbuscular mycorrhizal symbiosis in plants. *Cell Research* 24: 130–133.
- Zeng T, Holmer R, Hontelez J, Te Lintel-Hekkert B, Marufu L, de Zeeuw T, Wu F, Schijlen E, Bisseling T, Limpens E. 2018. Host- and stage-dependent secretome of the arbuscular mycorrhizal fungus *Rhizophagus irregularis*. *The Plant Journal* 94: 411–425.
- Zentella R, Zhang ZL, Park M, Thomas SG, Endo A, Murase K, Fleet CM, Jikumaru Y, Nambara E, Kamiya Y *et al.* 2007. Global analysis of della direct targets in early gibberellin signaling in *Arabidopsis*. *Plant Cell* 19: 3037–3057.
- Zhang ZL, Ogawa M, Fleet CM, Zentella R, Hu J, Heo JO, Lim J, Kamiya Y, Yamaguchi S, Sun TP. 2011. Scarecrow-like 3 promotes gibberellin signaling by antagonizing master growth repressor DELLA in *Arabidopsis*. *Proceedings of the National Academy of Sciences, USA* 108: 2160–2165.

Supporting Information

Additional Supporting Information may be found online in the Supporting Information section at the end of the article.

Fig. S1 β -glucuronidase (GUS) promoter–reporter analysis of *Medicago truncatula* MIG genes.

Fig. S2 *In silico* analysis of the promoter regions of *MIG1*, *MIG2* and *MIG3*.

Fig. S3 Ectopic expression of *MIG3* but not of *MIG2* negatively impacts arbuscule development.

Fig. S4 Amino acid alignment of the N-terminal region of MIG proteins.

Fig. S5 TPLATE is not regulated by *SCL3* or *MIG3*, while *CYC1* is regulated by both.

Fig. S6 MIG proteins require DELLA to control cortical cell width.

Fig. S7 *SCL3* is induced in arbuscule-containing cells and interacts with *MIG3*.

Fig. S8 Deregulation of *SCL3*.

Fig. S9 *SCL3*-like1 expression is not regulated by *SCL3* RNAi or MIGs.

Table S1 Shoot and root fresh weight and length for all performed experiments.

Table S2 Oligonucleotides and corresponding gene numbers for the genes analyzed in this study.

Table S3 Exact *P*-values of all experiments in this manuscript.

Please note: Wiley Blackwell are not responsible for the content or functionality of any Supporting Information supplied by the authors. Any queries (other than missing material) should be directed to the *New Phytologist* Central Office.



About New Phytologist

- *New Phytologist* is an electronic (online-only) journal owned by the New Phytologist Foundation, a **not-for-profit organization** dedicated to the promotion of plant science, facilitating projects from symposia to free access for our Tansley reviews and Tansley insights.
- Regular papers, Letters, Viewpoints, Research reviews, Rapid reports and both Modelling/Theory and Methods papers are encouraged. We are committed to rapid processing, from online submission through to publication 'as ready' via *Early View* – our average time to decision is <26 days. There are **no page or colour charges** and a PDF version will be provided for each article.
- The journal is available online at Wiley Online Library. Visit **www.newphytologist.com** to search the articles and register for table of contents email alerts.
- If you have any questions, do get in touch with Central Office (np-centraloffice@lancaster.ac.uk) or, if it is more convenient, our USA Office (np-usaoffice@lancaster.ac.uk)
- For submission instructions, subscription and all the latest information visit **www.newphytologist.com**